Modeling of electron spectra and of the total yield of backscattered and secondary electrons by electron impact

M. Dapor
ECT*
dapor@ectstar.eu

LEE2022 - 15.11.2022

Secondary Electron Energy Distribution (SEED):

A Monte Carlo program for simulating secondary and total electron emission

1. Theory

Monte Carlo method

Monte Carlo is a statistical method that can be used for evaluating the many physical quantities necessary to the study of the interactions of particle-beams with solid targets.

Letting the particles carry out an artificial, random walk – taking into account the effect of the single collisions – it is possible to accurately evaluate the diffusion process.

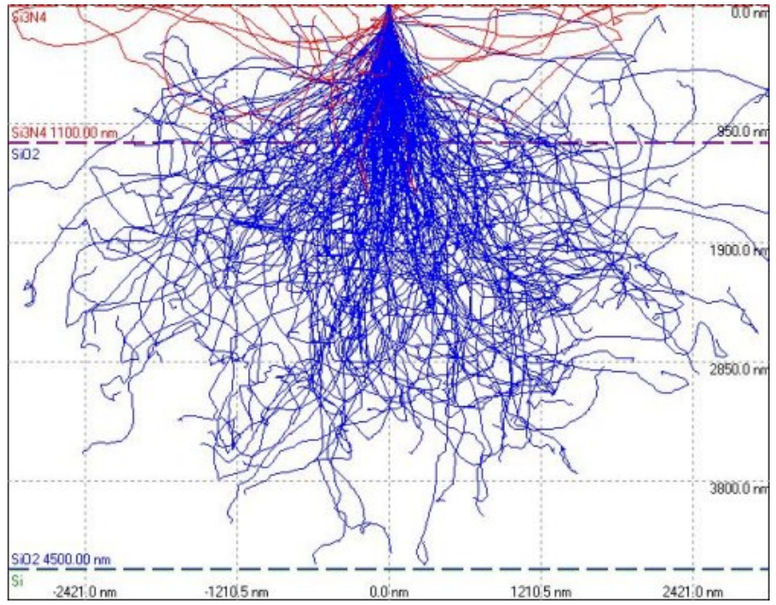

18 keV electrons striking a Si_3N_4 layer with a SiO_2 substrate (C. Walker, M. El Gomati)

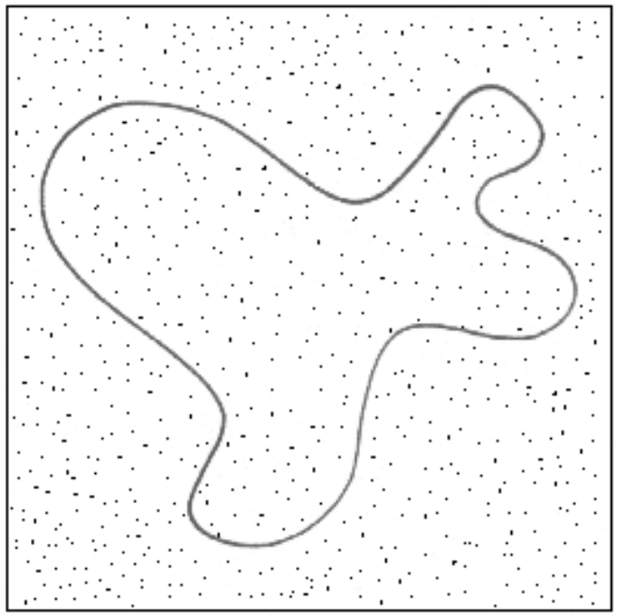

When the number of points is very large, the ratio of those fallen within the surface and the total number of points will approach the ratio between the (unknown) area of the surface and the (known) area of the square.

When the number of dimensions exceeds four, the Monte Carlo method is the best numerical procedure for the calculation of multiple integrals.

Generating pseudo-random numbers

Every number of the sequence of pseudo-random numbers is computable knowing the value of the last calculated random number:

$$\mu_{n+1} = (a\mu_n + b) \bmod m$$

where a, b and m are three integer ``magic'' numbers.

Choosing the values of the three ``magic'' numbers in a proper way, sequences of pseudo-random numbers are obtained.

Pseudo-random numbers distributed according to a given probability density

$$\int_a^{\xi} p(s)\, ds = \mu$$

ξ : random variable defined in a given range and distributed according to the probability density $p(s)$

μ : random variable uniformly distributed in the range [0,1]

Pseudo-random numbers distributed according to the exponential probability density

$$p_\chi(s) = \frac{1}{\lambda} \exp\left(-\frac{s}{\lambda}\right)$$

$$\mu = \int_0^\chi \frac{1}{\lambda} \exp\left(-\frac{s}{\lambda}\right)\, ds$$

$$\chi = -\lambda \ln(1 - \mu)$$

$1 - \mu$ and μ have the same distribution

$$\chi = -\lambda \ln(\mu)$$

λ : expected value of χ

Monte Carlo ingredients

A. Electron-atom interaction: elastic scattering cross-section

- Screened Rutherford cross-section
- Mott cross-section (relativistic partial wave expansion method)

B. Electron-atomic electron interaction: inelastic scattering cross-section

- Dielectric Ritchie's theory

C. Electron-phonon interaction: inelastic scattering cross-section

- Fröhlich's theory

D. Electron-polaron interaction: trapping phenomena

- Ganachaud and Mokrani semi-empiric model

Monte Carlo strategies

A.Continuous-slowing-down approximation

Step-length

$$\Delta s = -\lambda_{\mathrm{el}} \ln(\mu_1)$$

$$\lambda_{\mathrm{el}} = \frac{1}{N \sigma_{\mathrm{el}}}$$

$$\sigma_{\mathrm{el}}(E) = \int \frac{d\sigma_{\mathrm{el}}}{d\Omega}\, d\Omega = \int_0^{\pi} \frac{d\sigma_{\mathrm{el}}}{d\Omega}\, 2\,\pi\, \sin\vartheta\, d\vartheta$$

Polar scattering angle

$$P_{\mathrm{el}}(\theta, E) \;=\; \frac{2\,\pi}{\sigma_{el}} \int_0^{\theta} \frac{d\sigma_{\mathrm{el}}}{d\Omega}\, \sin\vartheta\, d\vartheta$$

$$\mu_2 \;=\; P_{\mathrm{el}}(\theta, E)$$

Direction of the electron after the last deflection

$$\cos\theta'_z \;=\; \cos\theta_z \cos\theta \;-\; \sin\theta_z \sin\theta\, \cos\phi$$

Energy loss

$$\Delta E = (dE/dz)\Delta z$$

With this approach, statistical fluctuations of the energy losses are completely neglected. As a consequence this kind of Monte Carlo strategy should be avoided when detailed information about energy loss mechanisms are required (for example when we are interested in the energy distribution of the emitted electrons).

B. Energy-straggling strategy

Step-length

$$\Delta s = -\lambda \, \ln(\mu_1)$$

$$\lambda = \frac{1}{N(\sigma_{\text{inel}} + \sigma_{\text{el}})}$$

$$\frac{1}{\lambda} = \frac{1}{\lambda_{\text{inel}}} + \frac{1}{\lambda_{\text{el}}}$$

Elastic and inelastic collisions

$$p_{\text{inel}} = \frac{\sigma_{\text{inel}}}{\sigma_{\text{inel}} + \sigma_{\text{el}}} = \frac{\lambda}{\lambda_{\text{inel}}}$$

$$p_{\text{el}} = 1 - p_{\text{inel}}$$

If a random number μ_2 is less than or equal to p_{inel}, then the collision will be inelastic; otherwise, it will be elastic.

Polar scattering angle

The polar scattering angle θ is calculated by generating a random number μ_3 , uniformly distributed in the range [0,1], representing the probability of elastic scattering into an angular range from 0 to θ:

$$\mu_3 = P_{\mathrm{el}}(\theta, E) = \frac{1}{\sigma_{el}} \int_0^{\theta} \frac{d\sigma_{el}}{d\Omega} 2\pi \sin\vartheta \, d\vartheta$$

Energy loss

The energy loss W is obtained by generating a random number μ_4 uniformly distributed in the range [0,1] and representing the probability of inelastic scattering into a range from 0 to W:

$$\mu_4 = P_{\text{inel}}(W, E) = \frac{1}{\sigma_{\text{inel}}} \int_0^W \frac{d\sigma_{\text{inel}}}{dw} dw$$

The energy-straggling strategy

$$\mu_2 < \frac{\lambda_{el}^{-1}}{\lambda_{el}^{-1}+\lambda_{inel}^{-1}}$$

yes

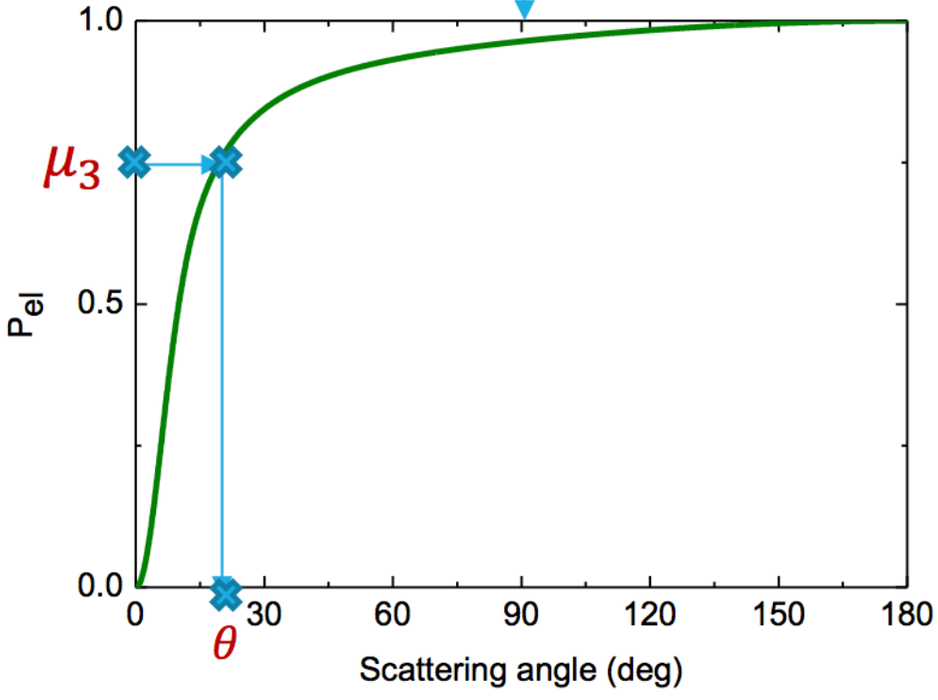

no

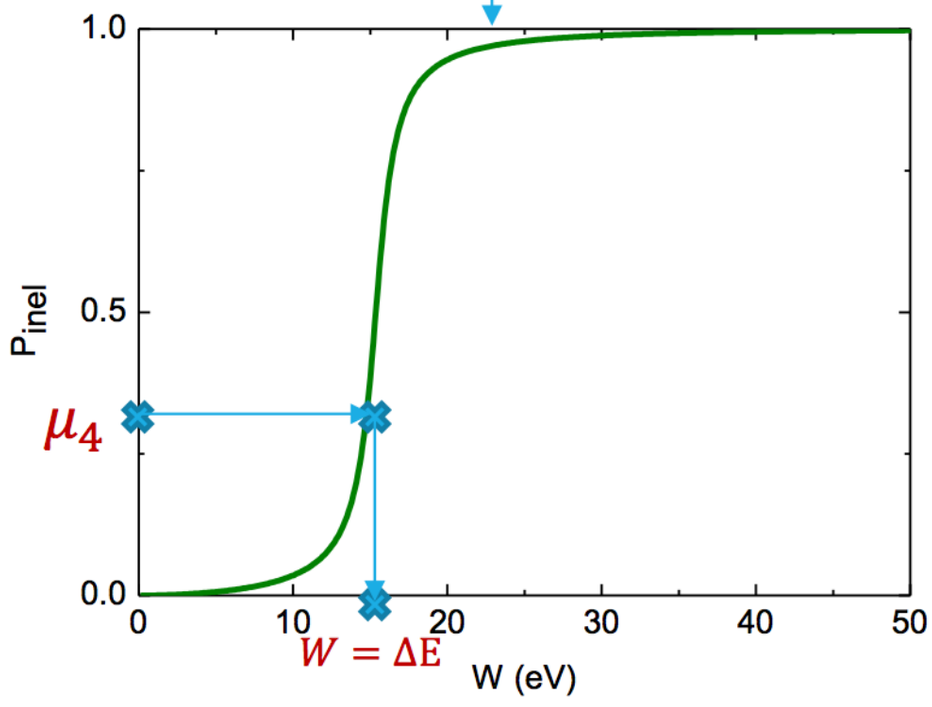

Electron-phonon interaction

If an electron-lattice interaction occurs, the energy lost by the electron is equal to the energy of the created phonon.

$$\lambda_{\text{phonon}} = \frac{\hbar\, k/m^*}{W_k^+}$$

Assuming $m^* = m$

$$\lambda_{\text{phonon}}^{-1} = \frac{1}{a_0}\,\frac{\varepsilon_0 - \varepsilon_\infty}{\varepsilon_0\ \varepsilon_\infty}\,\frac{W_{\text{ph}}}{E}\,\frac{n(T)+1}{2}\,\ln\left[\frac{1+\sqrt{1-W_{\text{ph}}/E}}{1-\sqrt{1-W_{\text{ph}}/E}}\right]$$

J. Llacer and E.I. Garwin, J. Appl. Phys. 40 (1965) 2766

Polaronic effect

A low-energy electron moving in an insulating material induces a polarization field that has a stabilizing effect on the moving electron. This phenomenon can be described as the generation of a quasi-particle called polaron.

$$\lambda_{\mathrm{pol}}^{-1} = C\, e^{-\gamma E}$$

C and γ are constant depending on the dielectric material.

J.P. Ganachaud and A. Mokrani, Surf. Sci. 334 (1995) 329

Polaronic effects

The electron ends its travel in the solid, as it is trapped where the interaction has taken place.

Electron-electron collisions: scattering angle

$$\sin\theta_s \;=\; \cos\theta$$

$$\frac{W}{E} \;=\; \frac{\Delta E}{E} \;=\; \sin^2\theta$$

Electron-phonon collisions: scattering angle

$$\cos\,\theta \;=\; \frac{E \,+\, E'}{2\,\sqrt{E\,E'}}\,(1 \,-\, B^{\mu_5}) \,+\, B^{\mu_5}$$

$$B \;=\; \frac{E \,+\, E' \,+\, 2\,\sqrt{E\,E'}}{E \,+\, E' \,-\, 2\,\sqrt{E\,E'}}$$

The interface with the vacuum represents a potential barrier, and not all the electrons that reach the surface can go beyond it. When a very slow electron reaches the target surface, it can emerge from the surface only if this condition is satisfied:

$$E \cos^2 \theta \geq \chi$$

χ is the electron affinity (semiconductors and insulators) or the work function (metals), i.e. the difference between the vacuum level and the bottom of the conduction band.

Transmission coefficient

The MC code permits the electron to be emitted into the vacuum if the condition:

$$\mu_6 < \frac{4\sqrt{1-\chi/(E\,\cos^2\theta)}}{[1+\sqrt{1-\chi/(E\,\cos^2\theta)}]^2}$$

(where μ_6 is a random number uniformly distributed in the range [0,1]) is satisfied.
Those electrons which, once reached the surface, do not satisfy the condition to emerge, are reflected back into the bulk of the specimen without energy loss.

A. Messiah, Quantum Mechanics (North-Holland, Amsterdam, 1961)

2. Applications

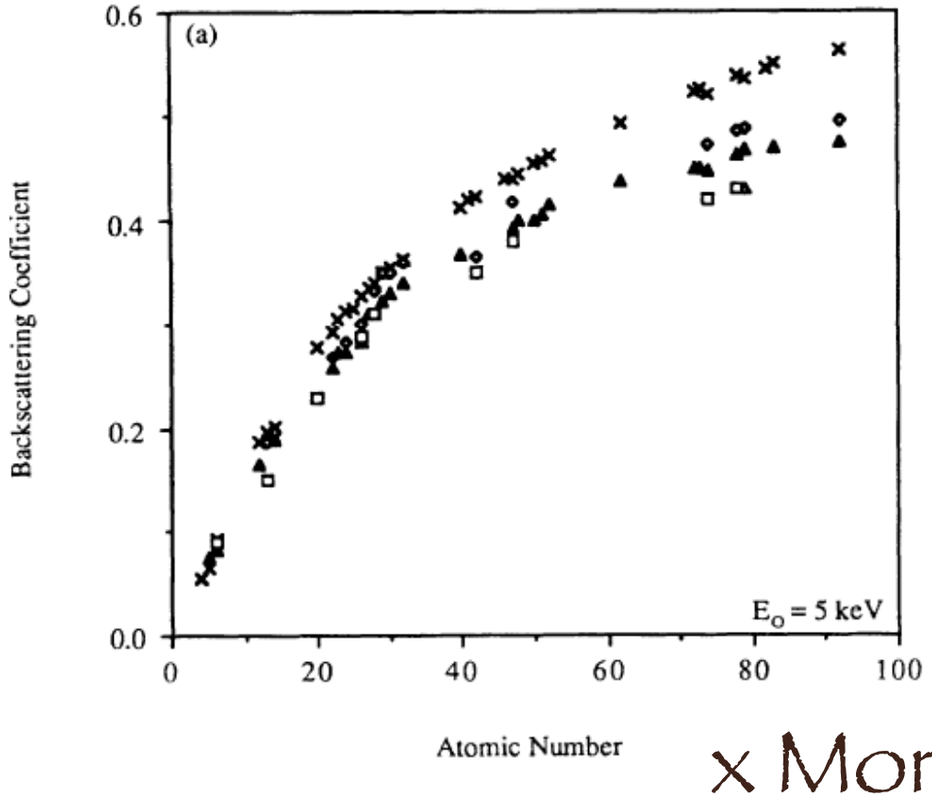

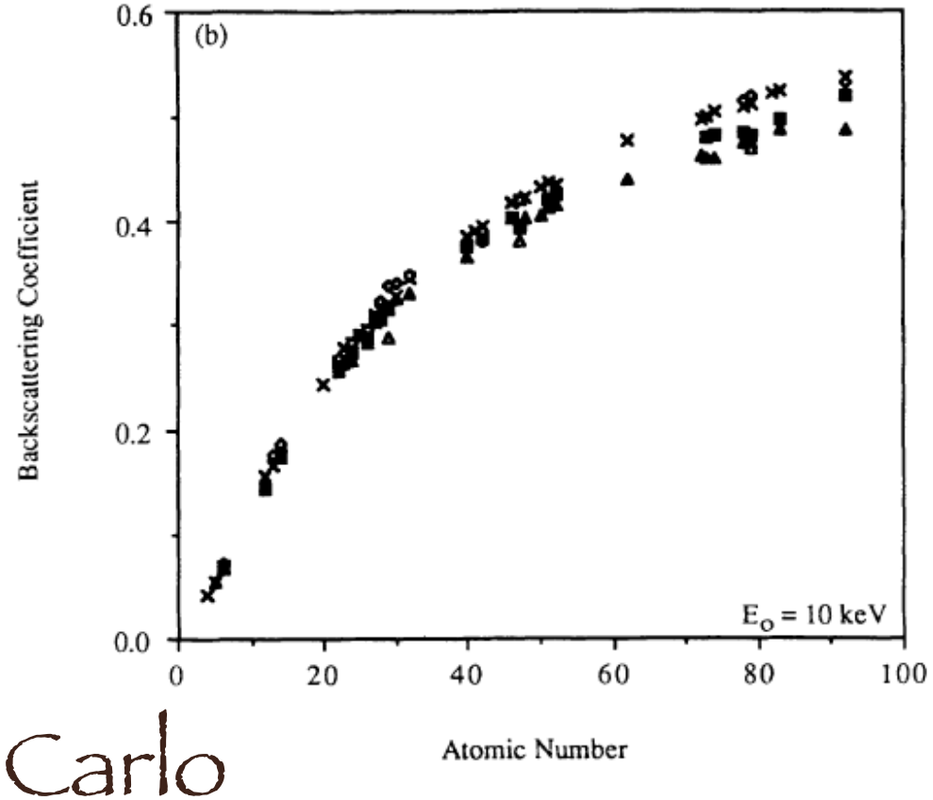

x Monte Carlo

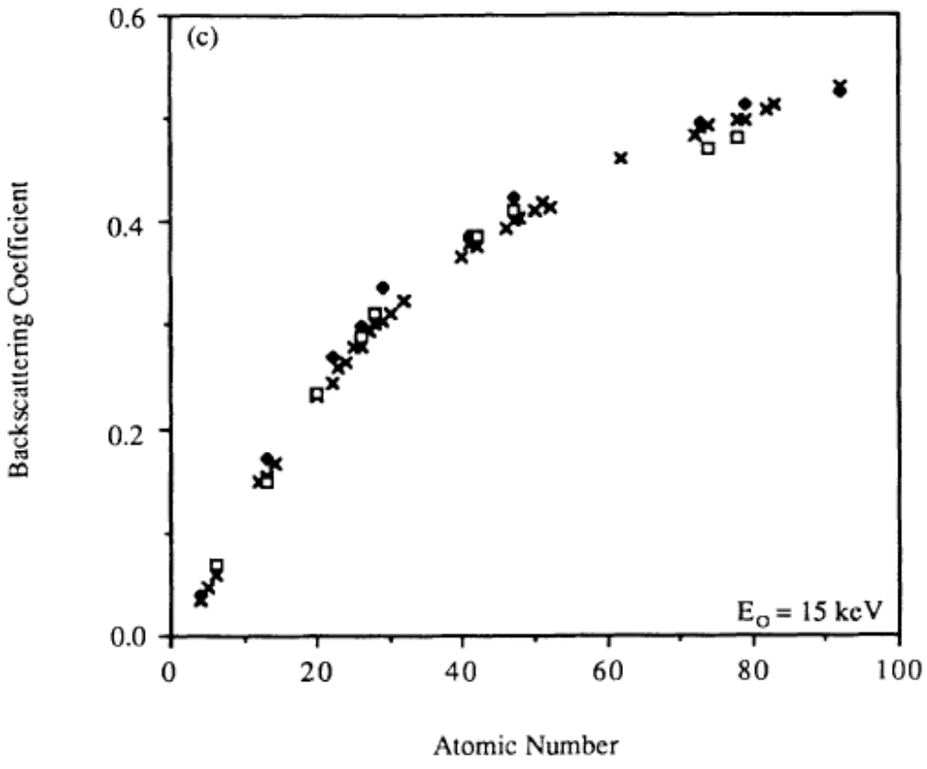

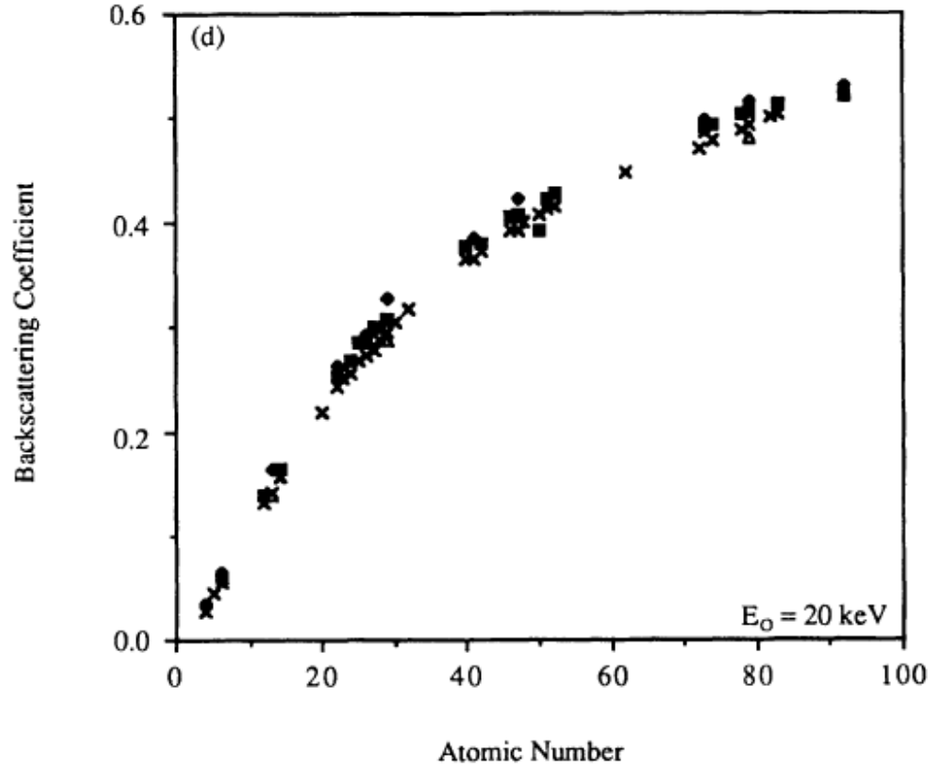

M. Dapor, Phys. Rev. B 46 (1992) 618

A comparative study of electrons and positrons

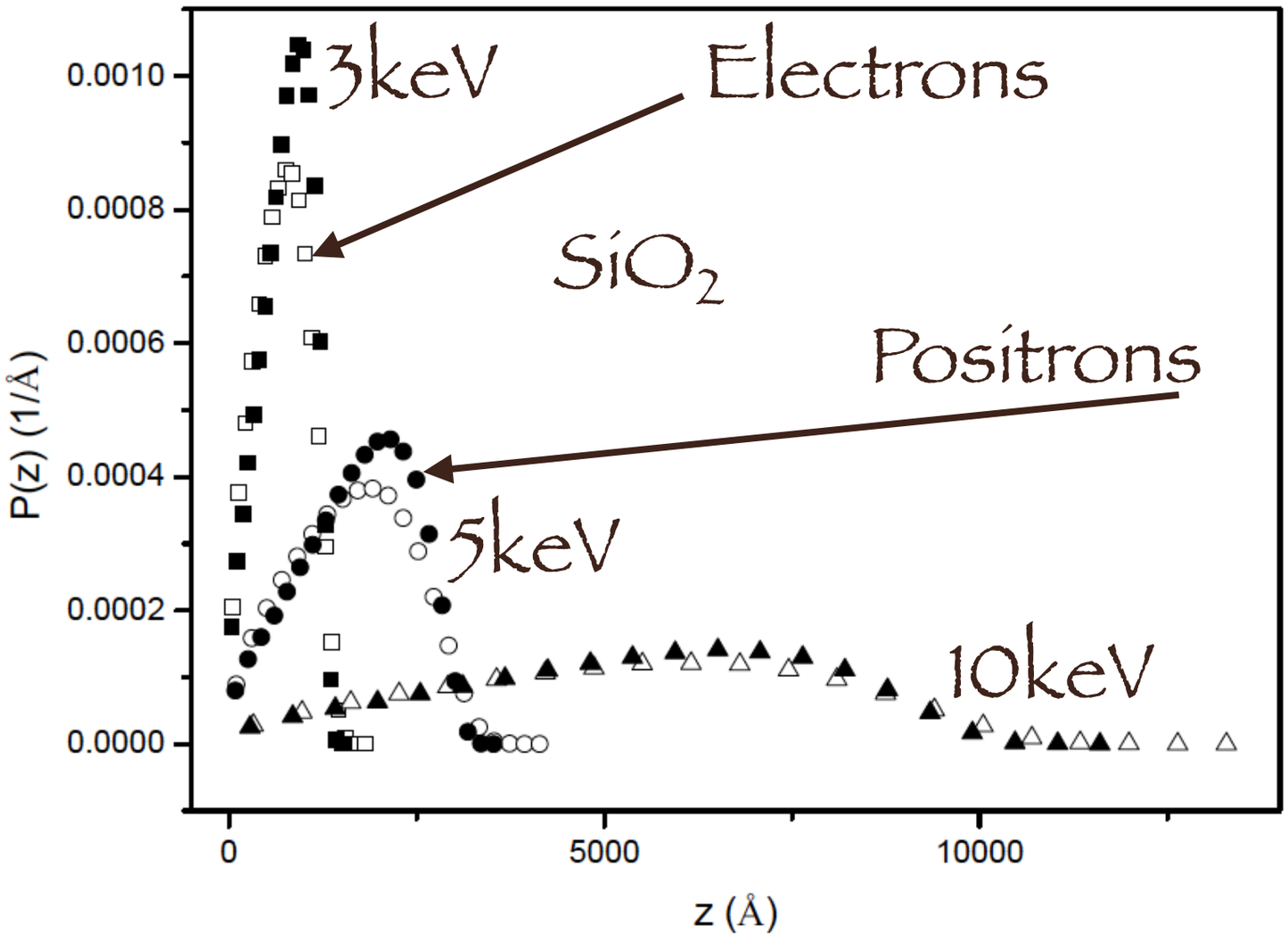

M. Dapor, J. Electron Spectrosc. Relat. Phenomena 151 (2006) 182

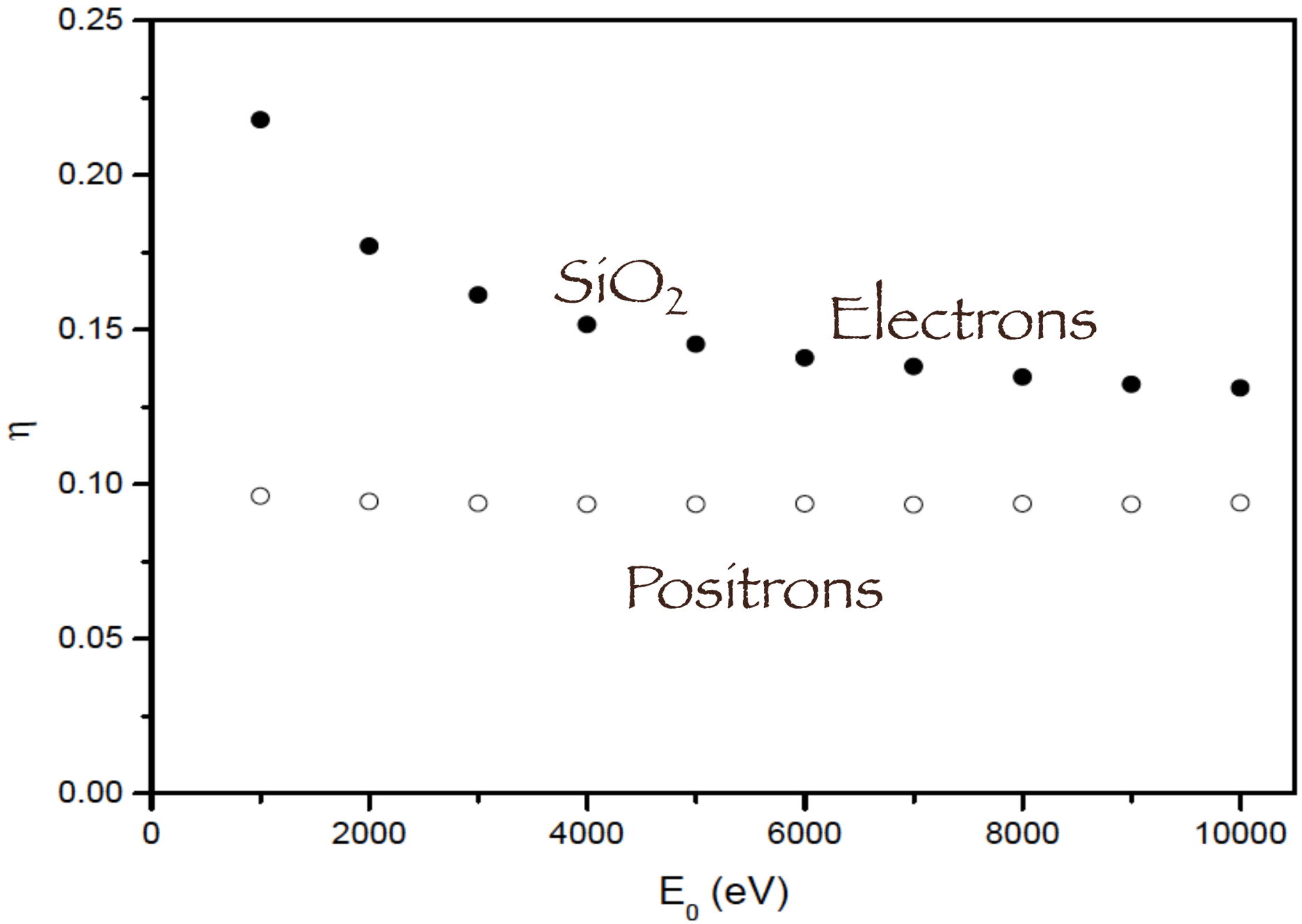

M. Dapor, J. Electron Spectrosc. Relat. Phenomena 151 (2006) 182

e- -> Al_2O_3

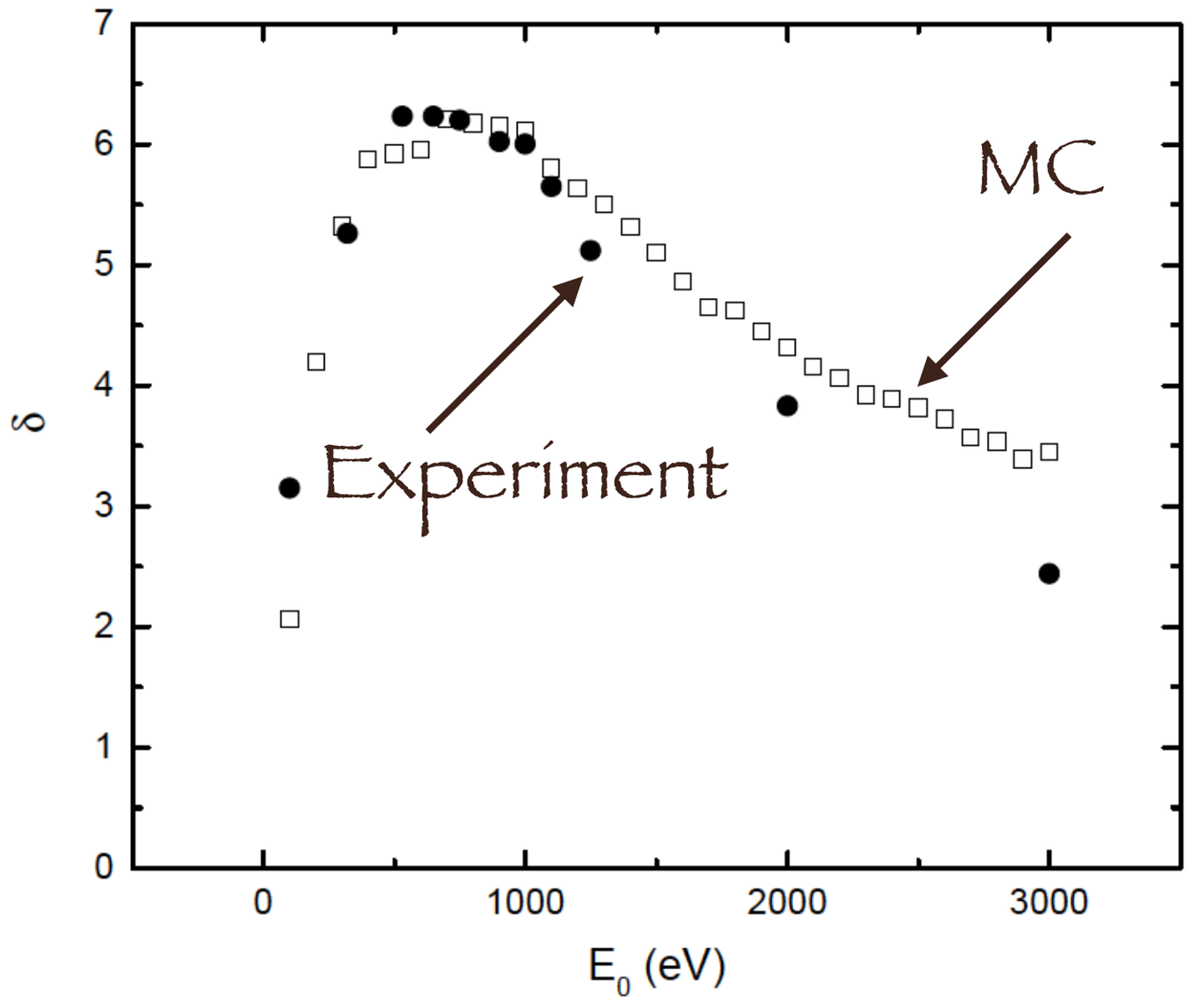

M. Dapor, Nuclear Instrum. Meth. Phys. Res. B 269 (2011) 1668

e- -> PMMA

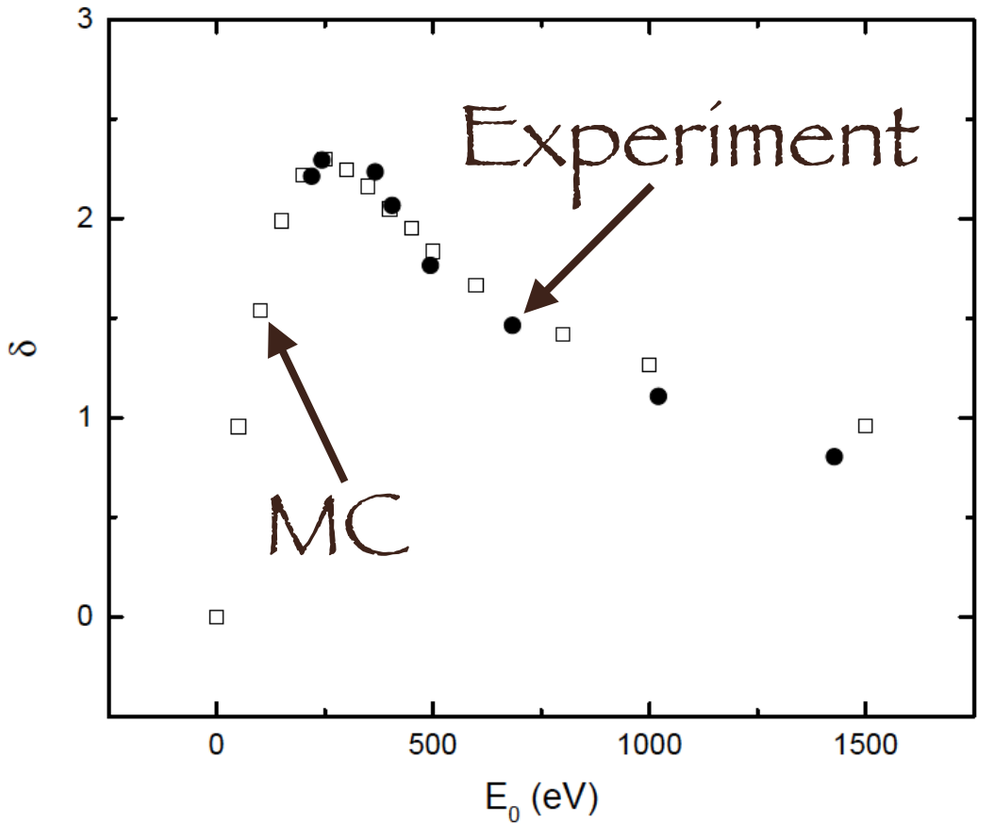

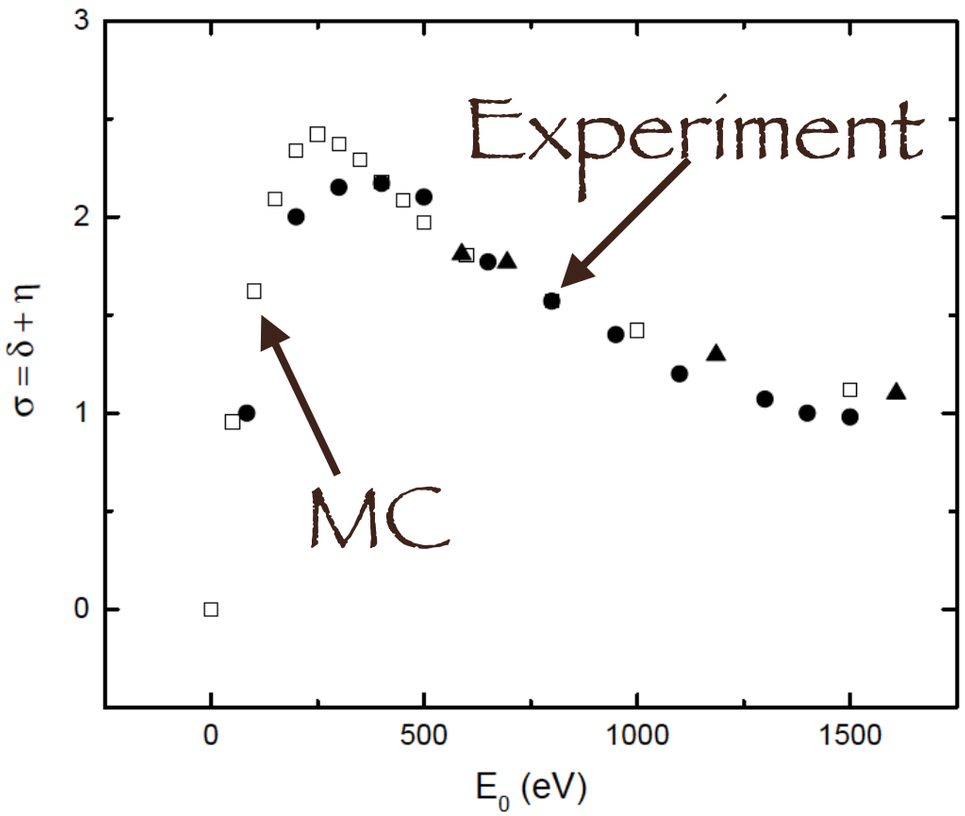

M. Dapor, Applied Surface Science 391 (2017) 3

e- -> Cu, Ag, Au

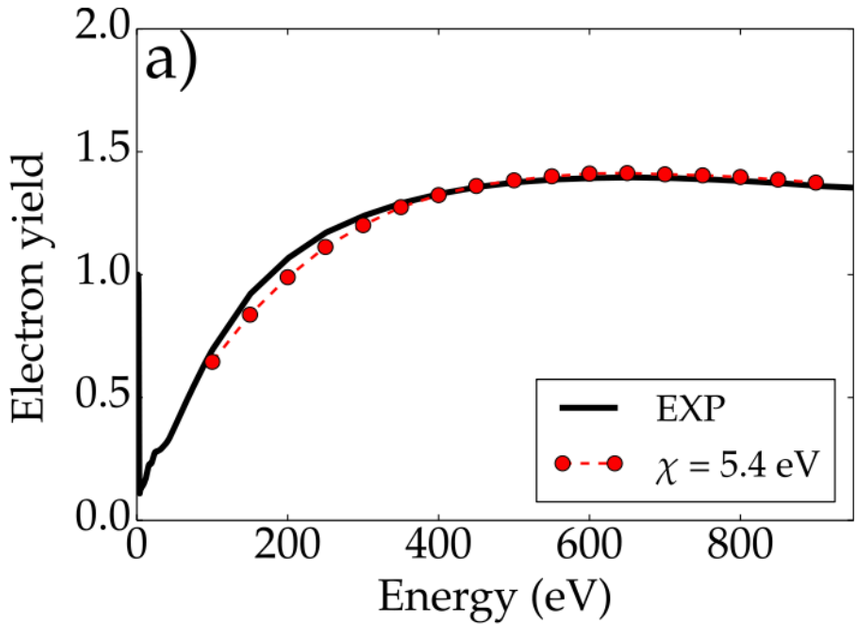

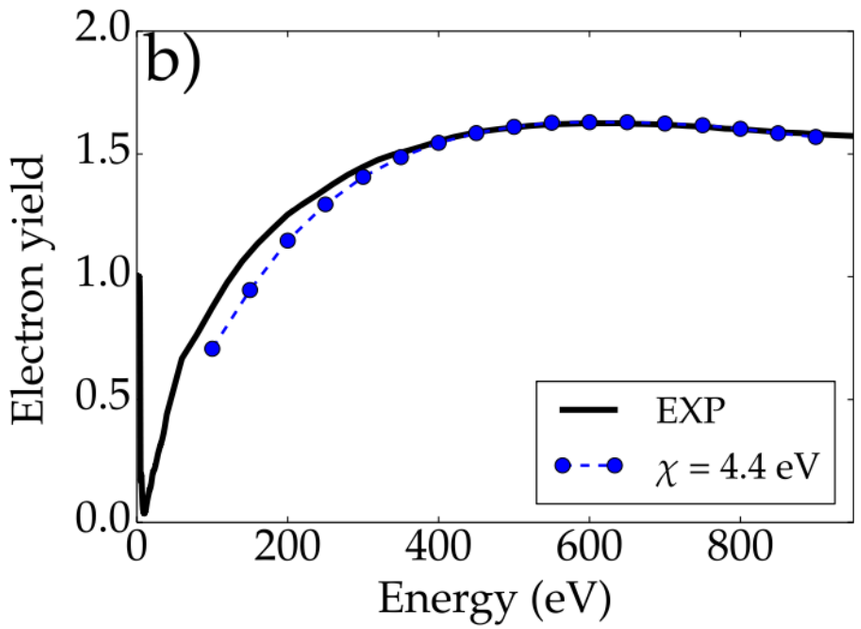

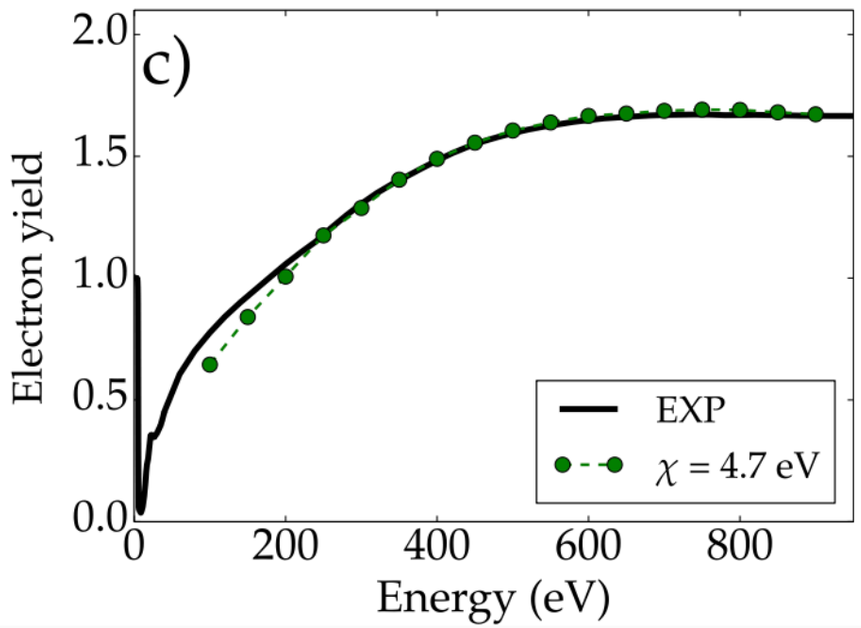

Electron yield curves of (a) Cu, (b) Ag, and (c) Au as a function of the initial primary electron beam kinetic energy .

M. Azzolini, M. Angelucci, R. Cimino, R. Larciprete, N. M. Pugno, S. Taioli, M. Dapor, J. Phys.: Condens. Matter 31 (2019) 055901

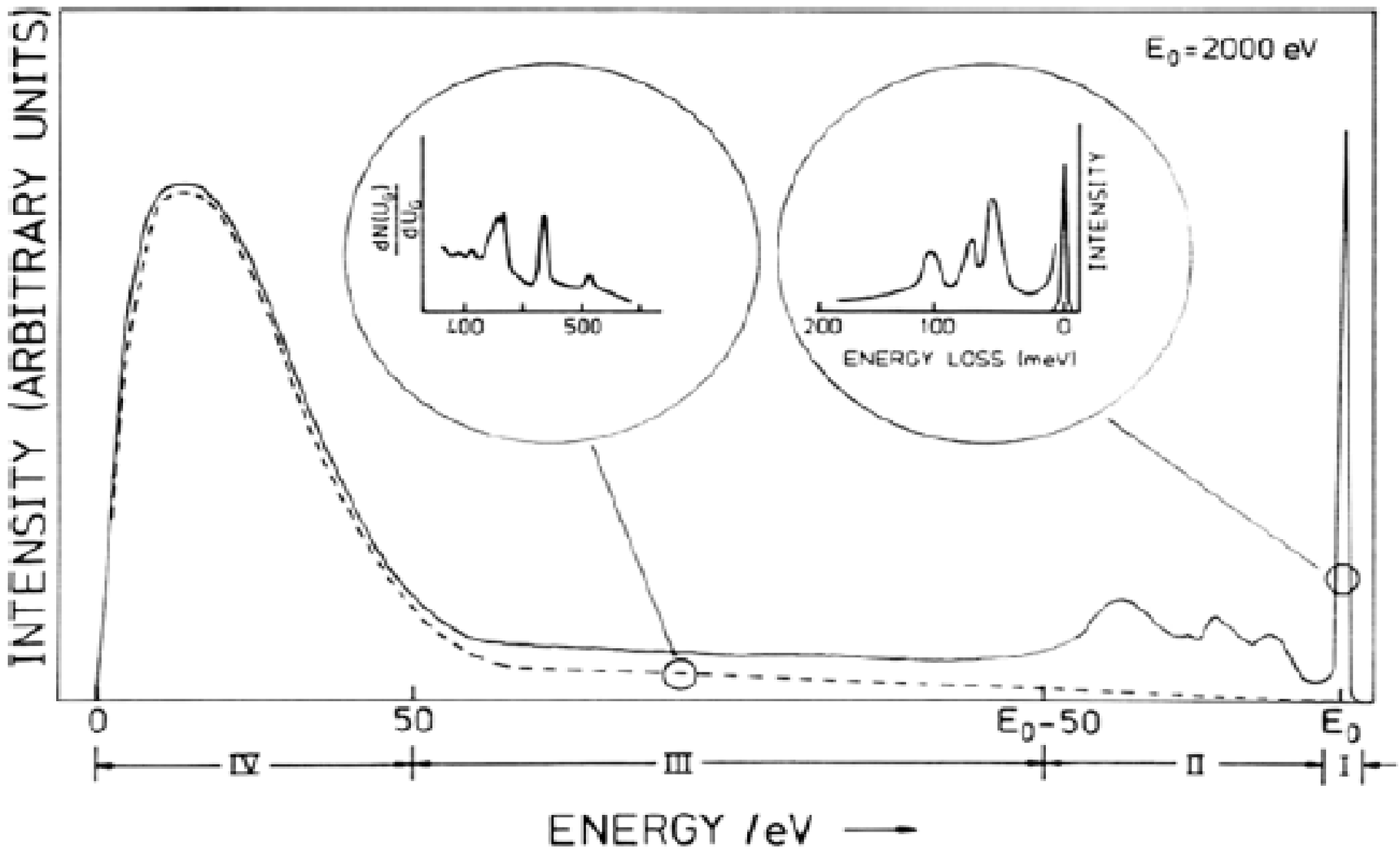

Electron energy distribution spectrum, including both primary and secondary processes, showing the elastic peak (I) and phonon losses (inset), plasmon-loss peaks (II), core-electron excitations (III) resulting in Auger processes (inset) and the peak of low energy secondary electrons (IV).From H. Ibach Electron Spectroscopy for Surface Analysis, Springer, Berlin, Heidelberg (1977)

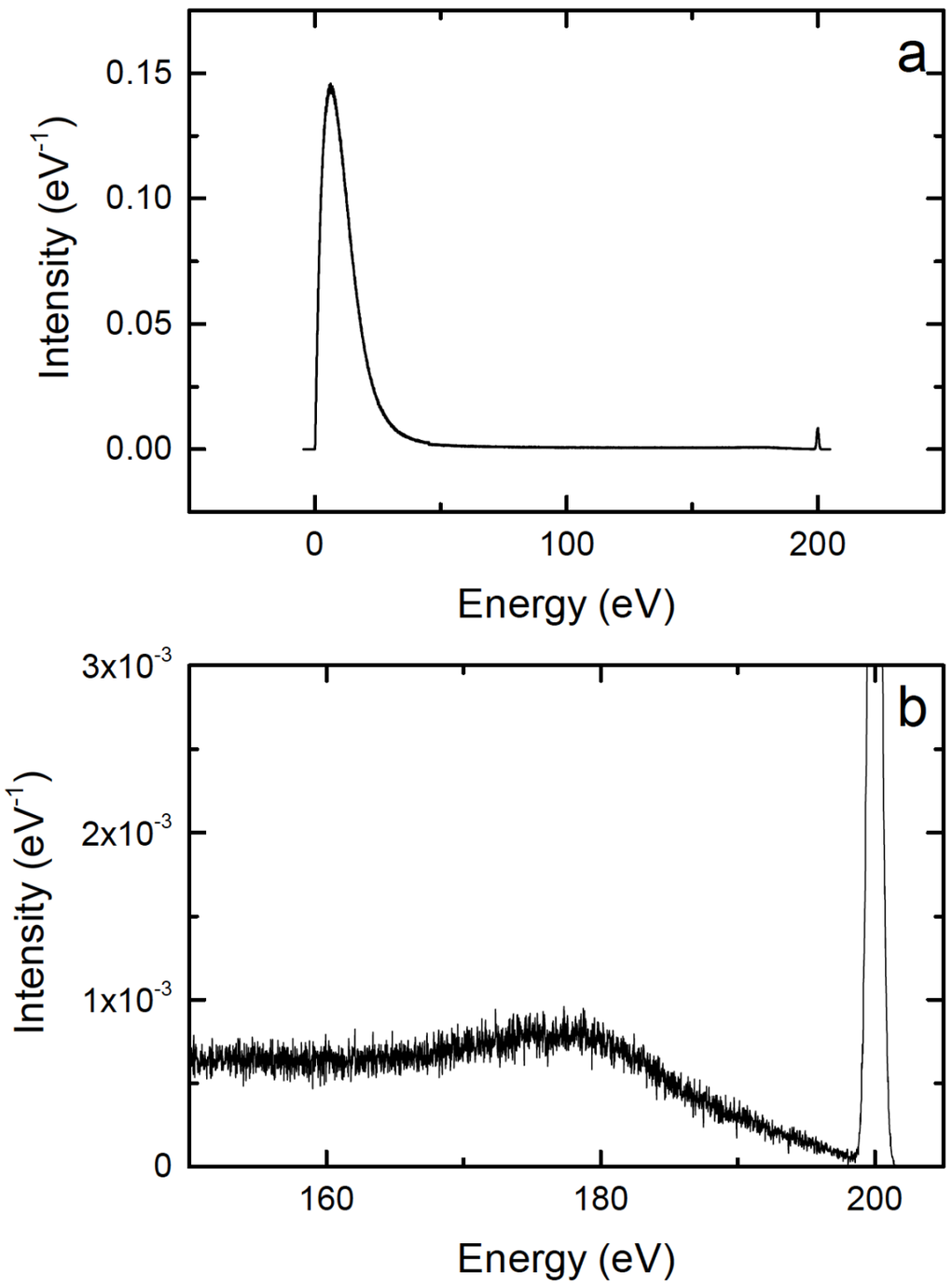

Monte Carlo simulation of the PMMA spectrum (E_0 ≈ 200eV)

M. Dapor, Applied Surface Science 391 (2017) 3

PMMA

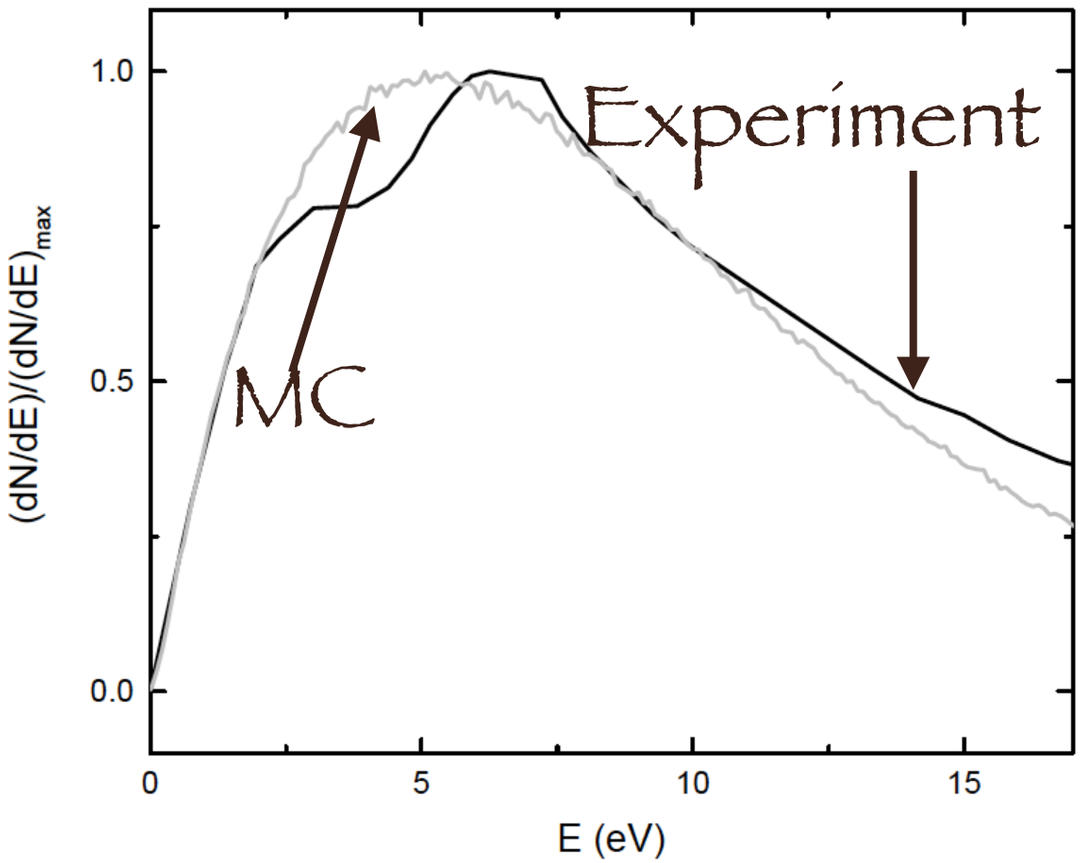

Monte Carlo simulation of the secondary electrons emitted by a PMMA target (E_0 = 1000eV)

M. Dapor, Applied Surface Science 391 (2017) 3

HOPG

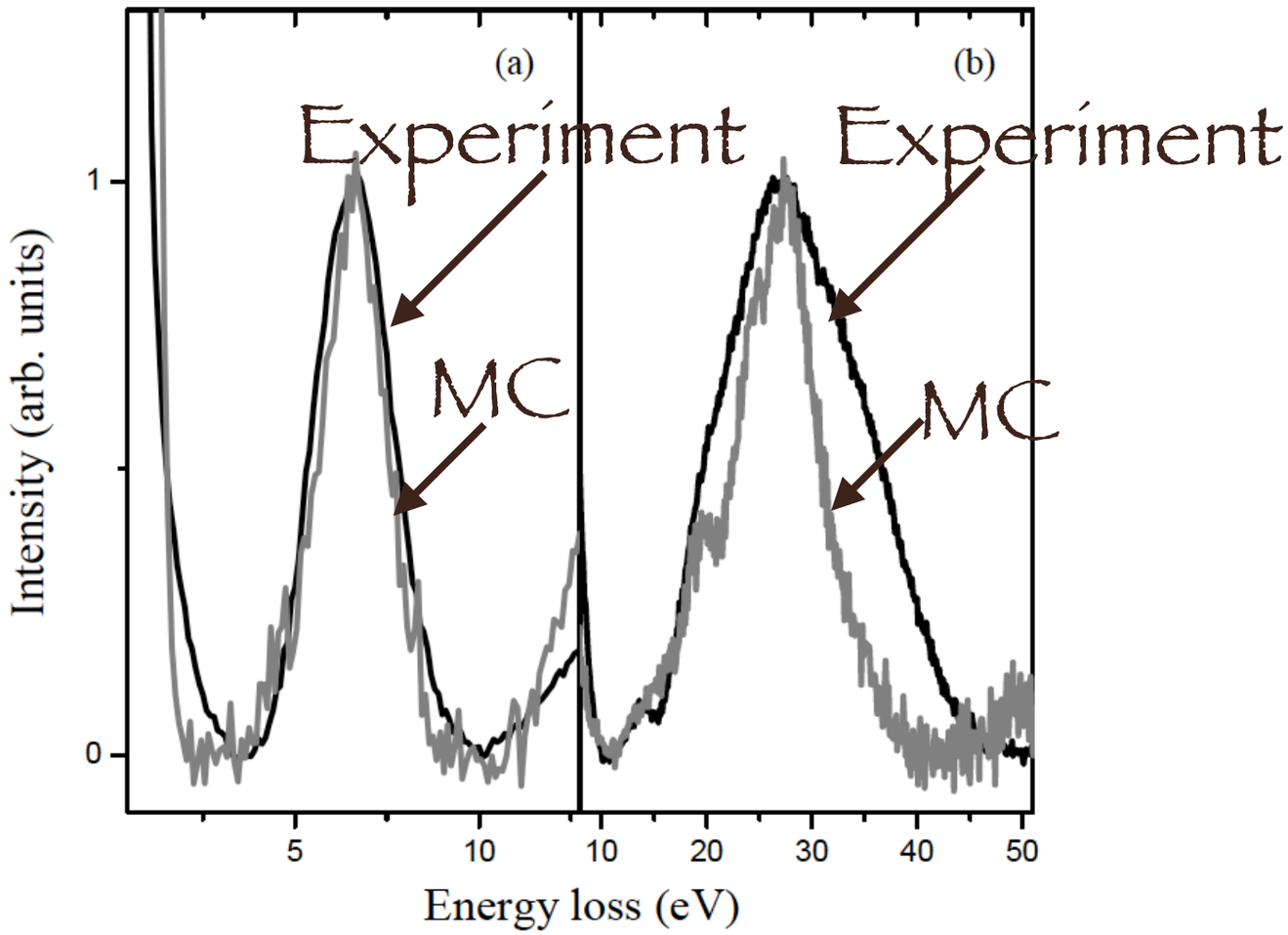

Monte Carlo simulation of the plasmon loss peaks of Highly Oriented Pyrolitic Graphite (HOPG) (E_0 = 500eV)

M. Dapor, L. Calliari, M. Filippi, Nuclear Instrum. Meth. Phys. Res. B 255 (2007) 276

SiO_2

Optical data

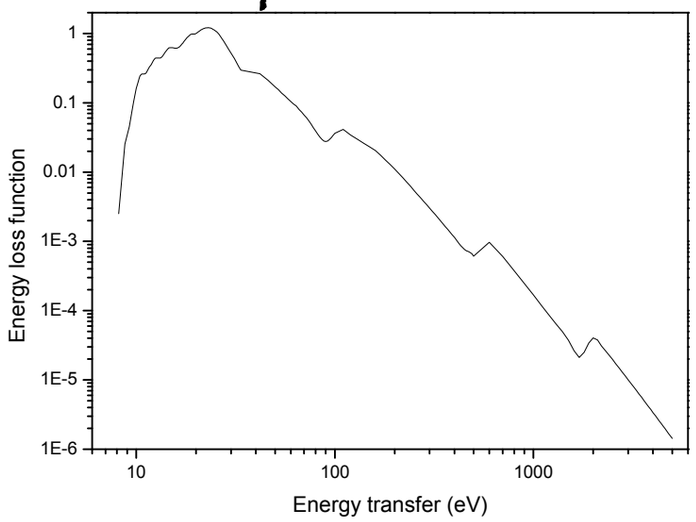

U. Buechner (1975)

B.L. Henke et. al. (1993)

REEL Spectrum

Primary energy: 2 keV

red line: experiment

green line: Monte Carlo

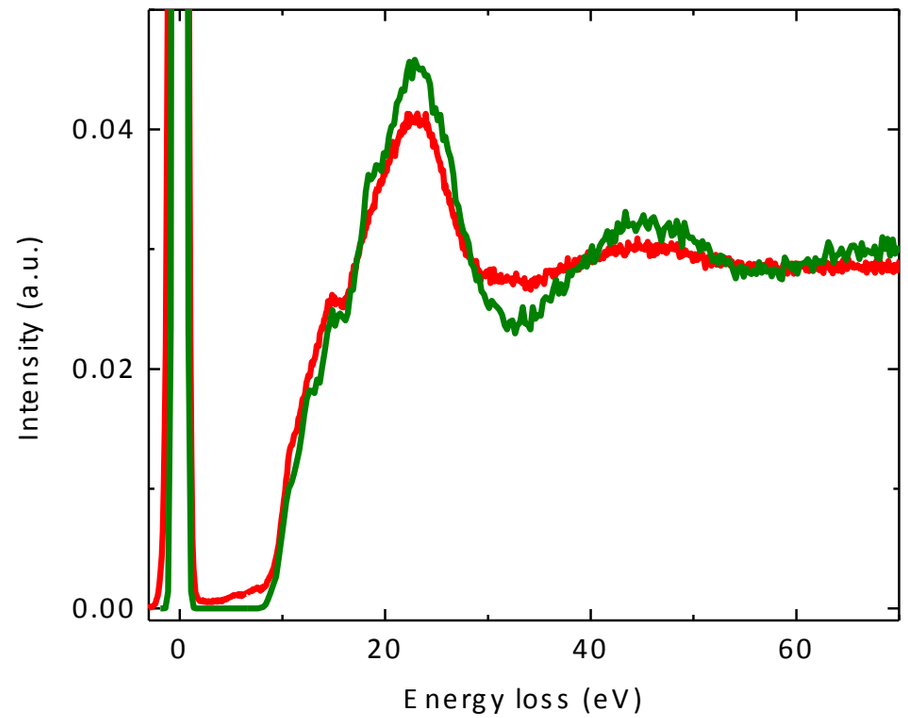

	REELS E_0=90 eV	REELS E_0=2 keV	MC E_0=2 keV
Band gap	8.3	8.9	9
T1	10.6	10.7	10.5
T2	12.9	12.6	12.3
T3	14.7	14.6	14.9
T4	17.7	18.8	18.4
Plasmon	21.1	22.9	23

Collective excitations and interband transitions

M. Filippi, L. Calliari, M. Dapor, Phys. Rev B 75 (2007) 125406

Surface effects

The surface is an interface between the bulk of the material and the vacuum. Since the dielectric function depends on the material, we expect the mean energy of the plasmons characterizing the surface (surface plasmons) to be different from the mean energy of the bulk plasmons.

Chiarello et al. observed that the REEL spectrum can be described by the combination of two terms, arising from surface and bulk inelastic scattering.

$$f_b(k,\omega) \;=\; \mathrm{Im}\left[\frac{-1}{\varepsilon(k,\omega)}\right] \qquad \text{bulk}$$

$$f_s(k,\omega) \;=\; \mathrm{Im}\left[\frac{-1}{\varepsilon(k,\omega)\;+\;1}\right] \qquad \text{surface}$$

G. Chiarello, E. Colavita, M. De Crescenzi, S. Nannarone, Physical Review B, 29 (1984) 4878

Region where surface plasmons are excited

$$-v/2\omega_s \leq z \leq v/2\omega_s$$

$$\omega_s = \frac{\omega_p}{\sqrt{2}}$$

$v =$ electron velocity

Z.J. Ding, H.M. Li, Q.R. Pu, Z.M. Zhang, R. Shimizu, Phys. Rev. B 66 (2002) 085411

W.S.M. Werner, Phys. Rev. B 74 (2006) 075421

M. Vicanek, Surf. Sci. 440 (1999) 1

Simulated REEL spectra for 1-10 keV electrons impinging on Al

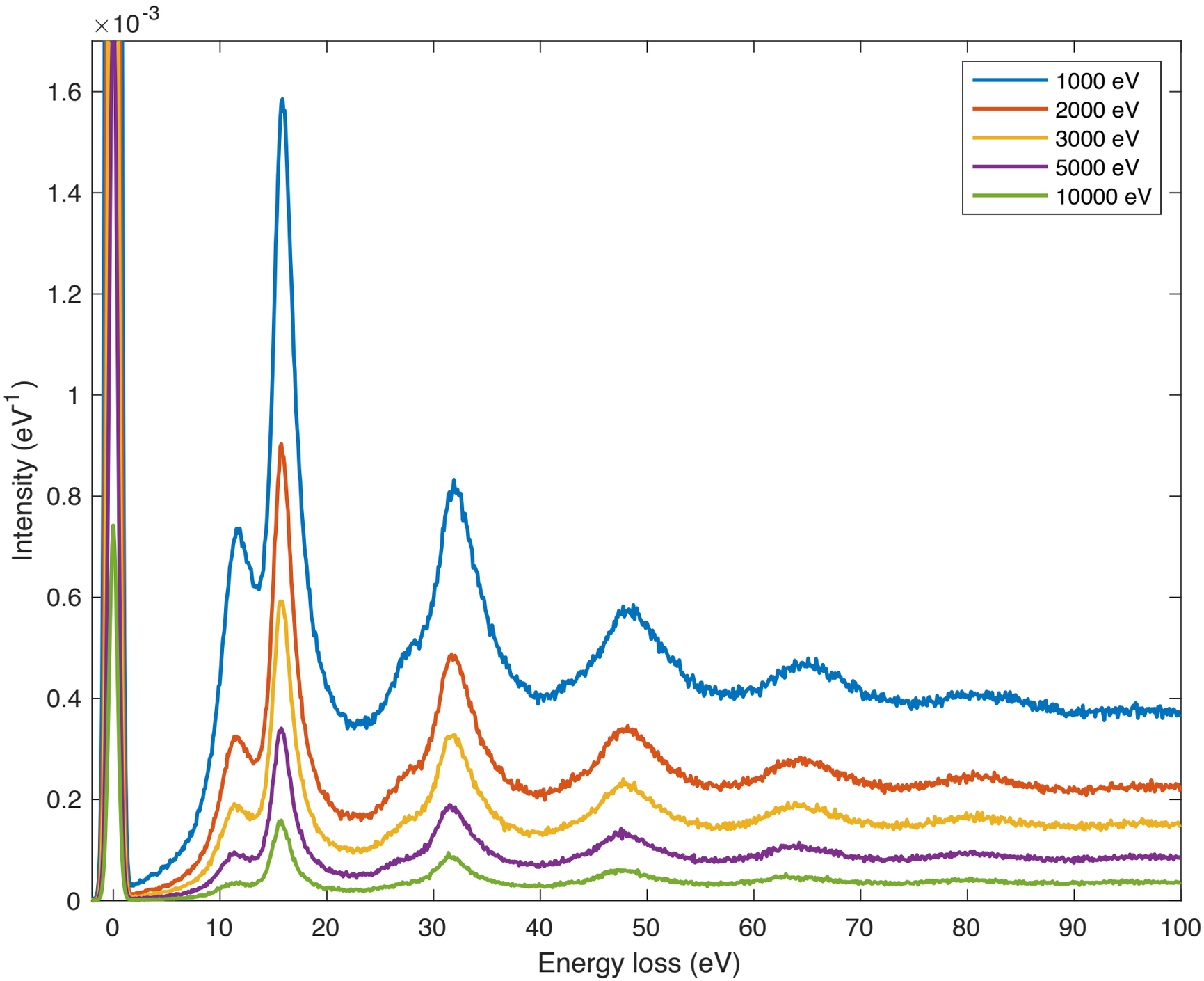

M. Dapor, Frontiers in Materials, in press

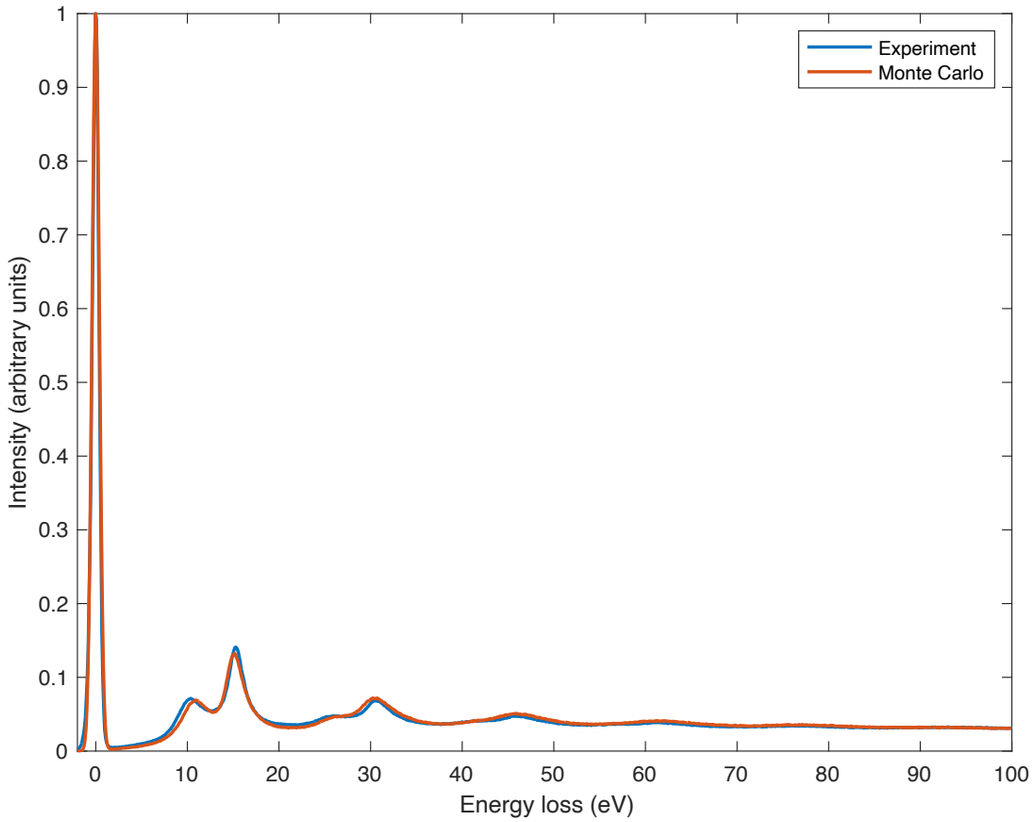

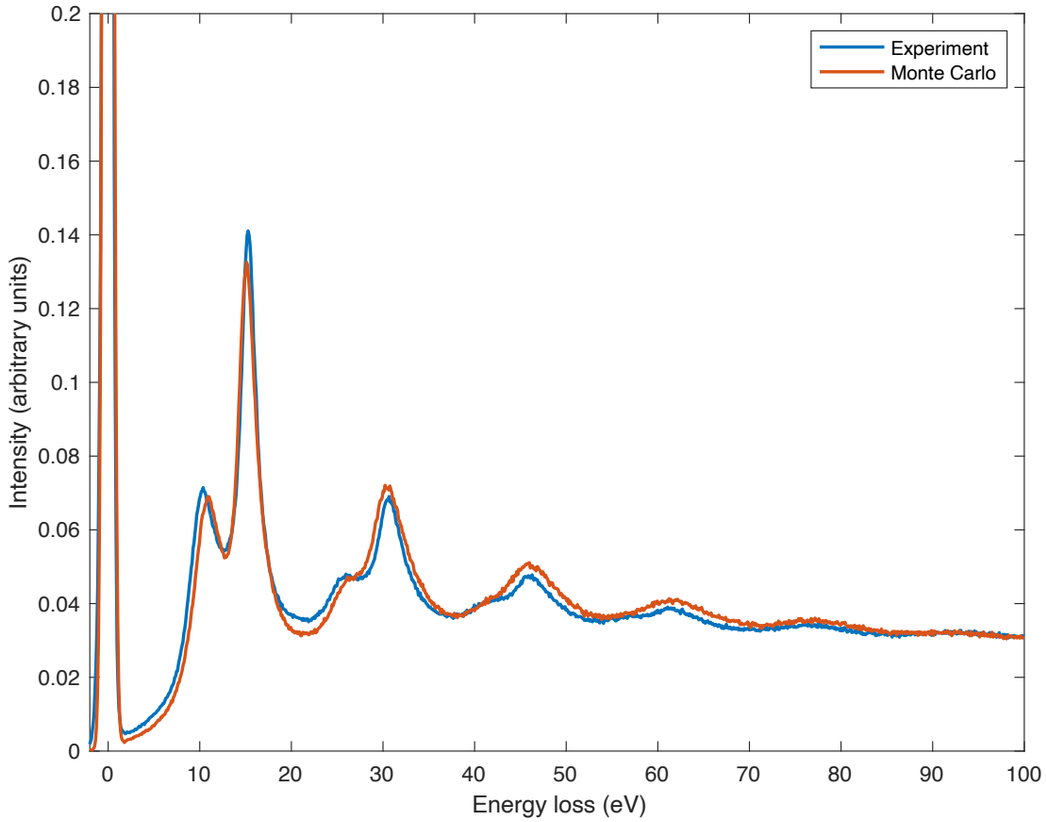

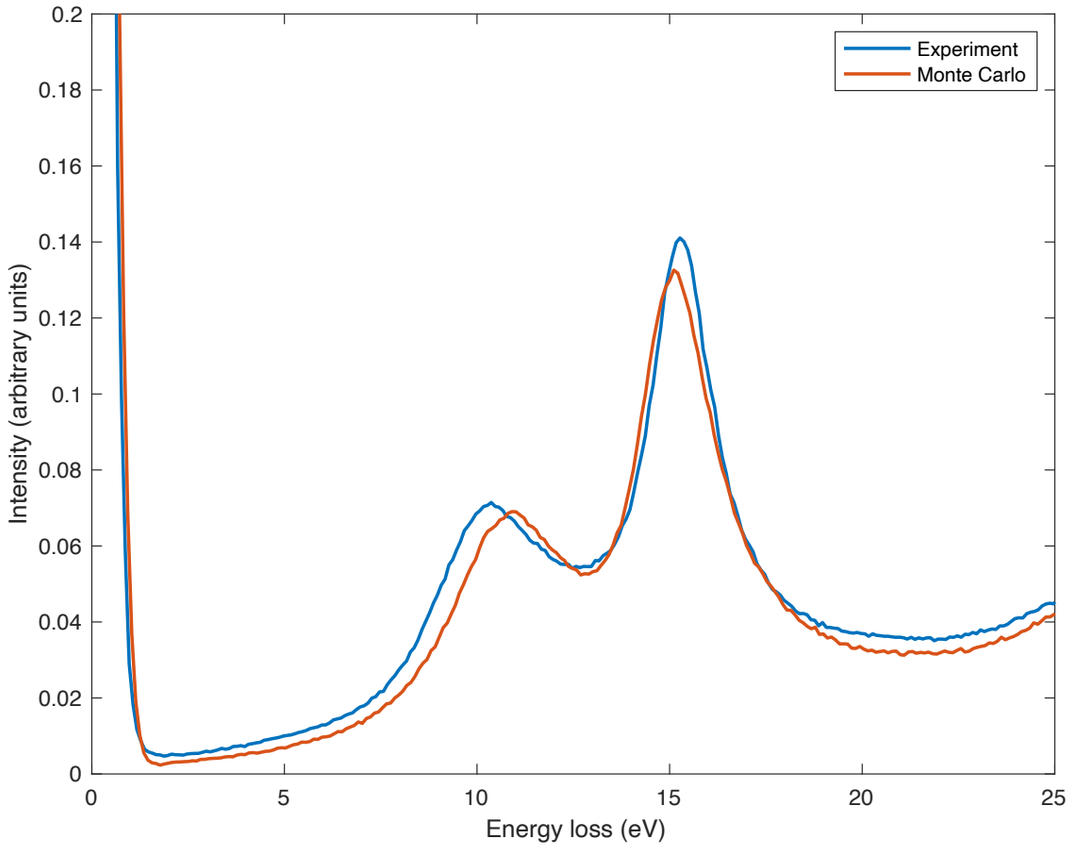

Experimental and simulated REEL spectra for 1000 eV electrons impinging on Al. The spectra were normalized to a common area of the zero-loss peak.

M. Dapor, Frontiers in Materials, in press

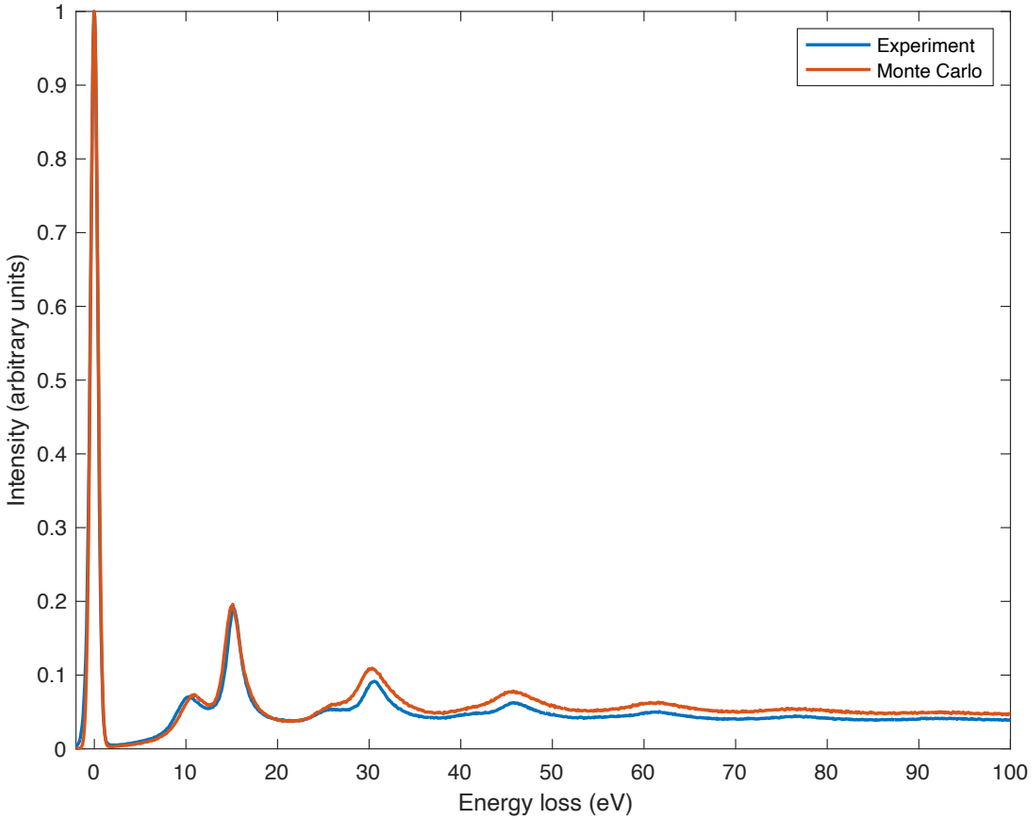

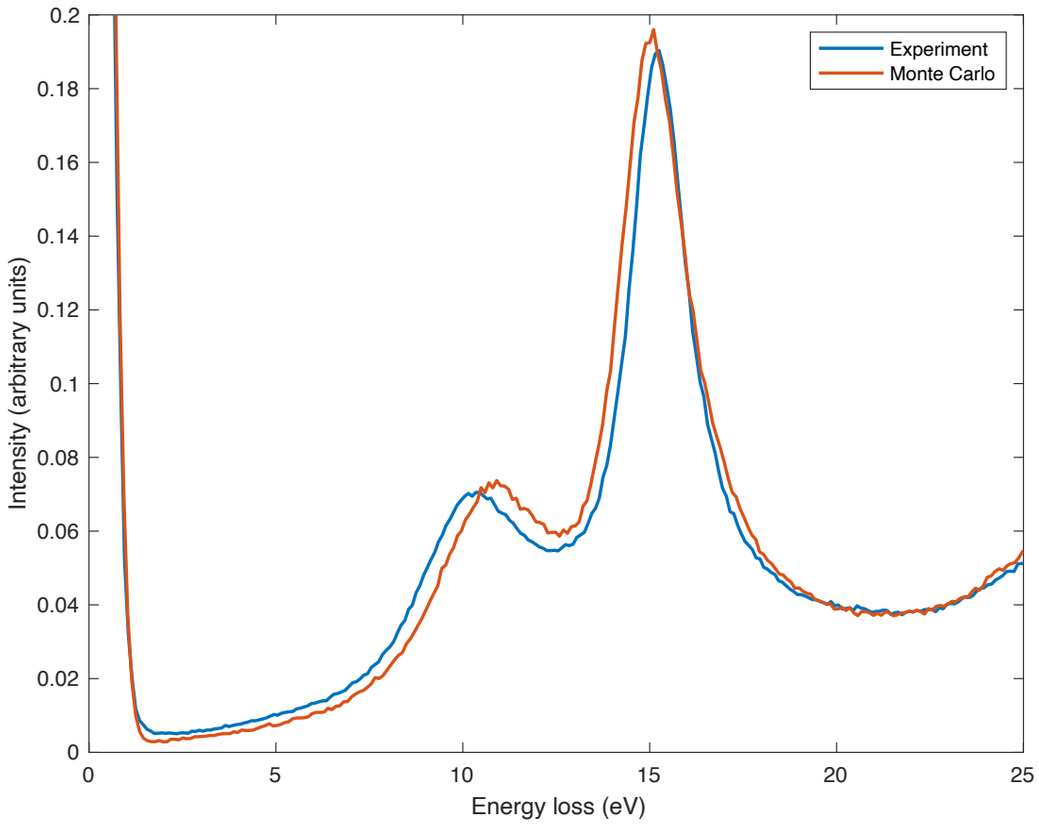

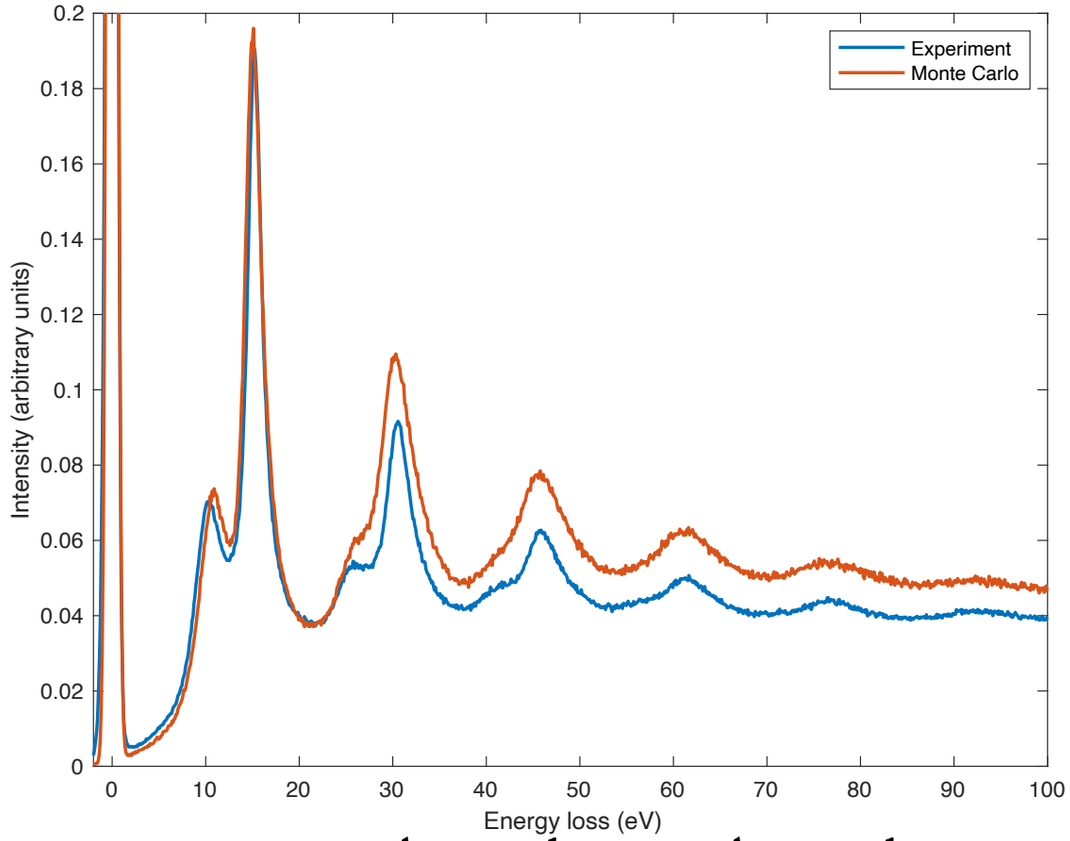

Experimental and simulated REEL spectra for 2000 eV electrons impinging on Al. The spectra were normalized to a common area of the zero-loss peak.

M. Dapor, Frontiers in Materials, in press

Energy loss of Auger electrons

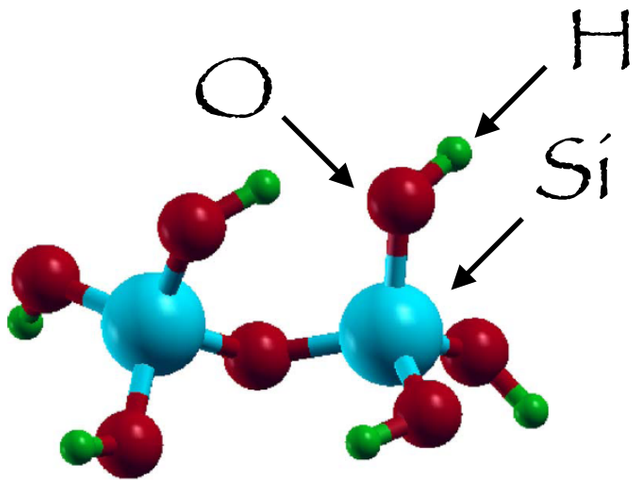

Sketch of the $Si_2O_7H_6$ nano-cluster optimized structure, used for the quantum mechanical calculations.

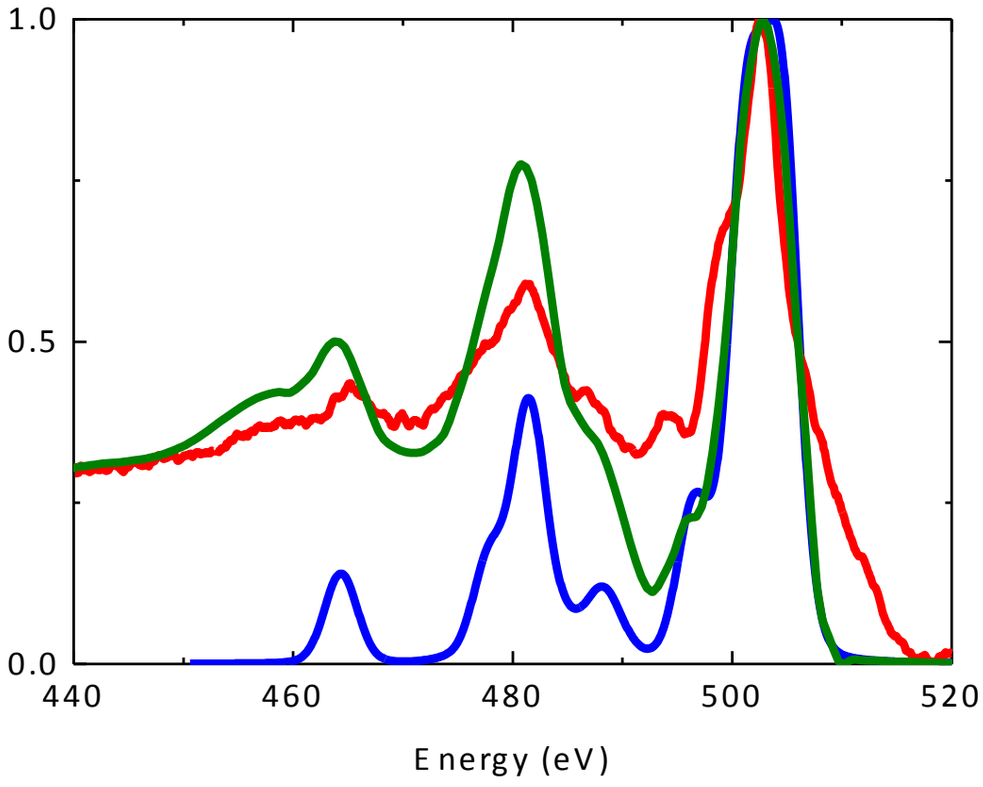

O K-LL Auger spectrum in SiO2. Experimental data (red line. Quantum mechanical theoretical data (blue line. Monte Carlo results (green line).

S. Taioli, S. Simonucci, L. Calliari, M. Filippi, M. Dapor, Phys. Rev. B 79 (2009) 085432

Doped Si

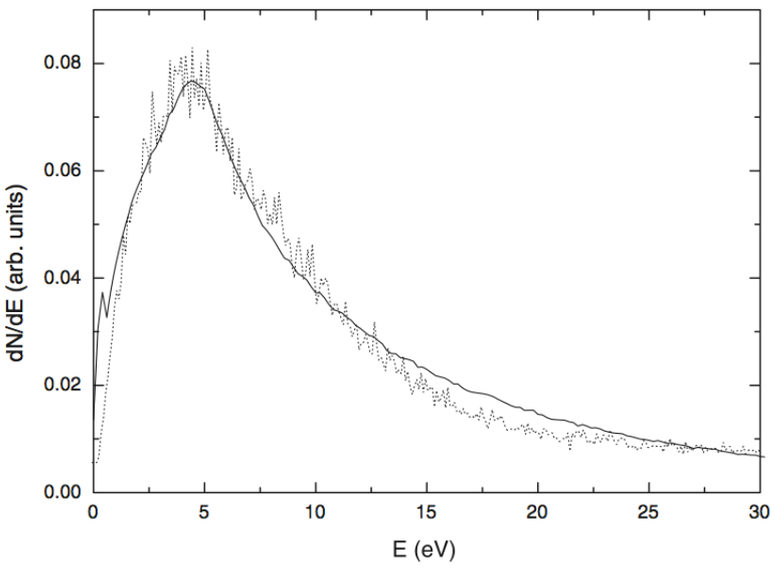

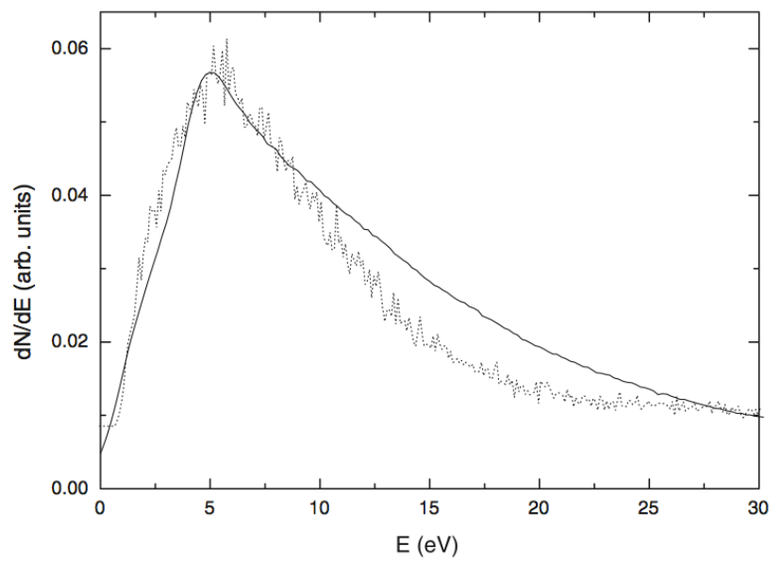

p-type silicon target

(p doping = 3 × 10^{18} cm^{-3})

n-type silicon target

(n doping=5× $10^{18}$$cm^{-3}$)

Solid line: experimental data (J. Castle et al.)

Dotted line: Monte Carlo results

M. Dapor, B. Inkson, C. Rodenburg, J.M. Rodenburg, EPL, 82 (2008) 30006

$$C_{pn} = \frac{I_p - I_n}{I_p + I_n}$$

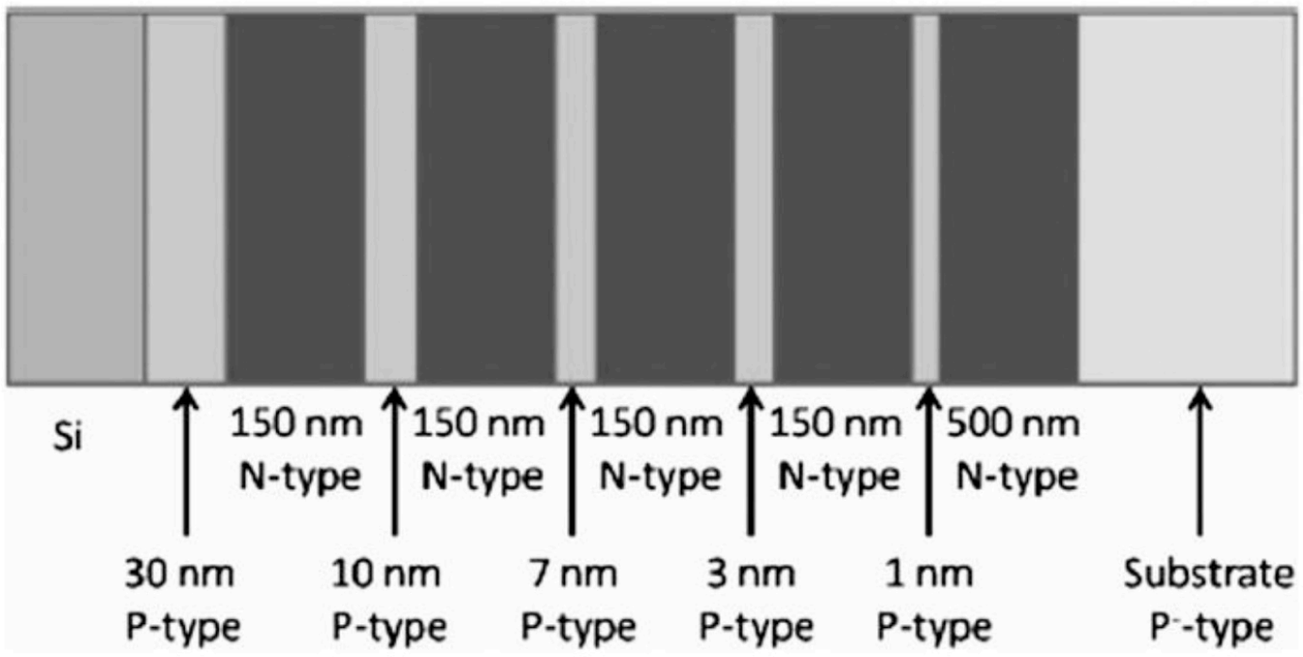

Schematic drawing of resolution test structure

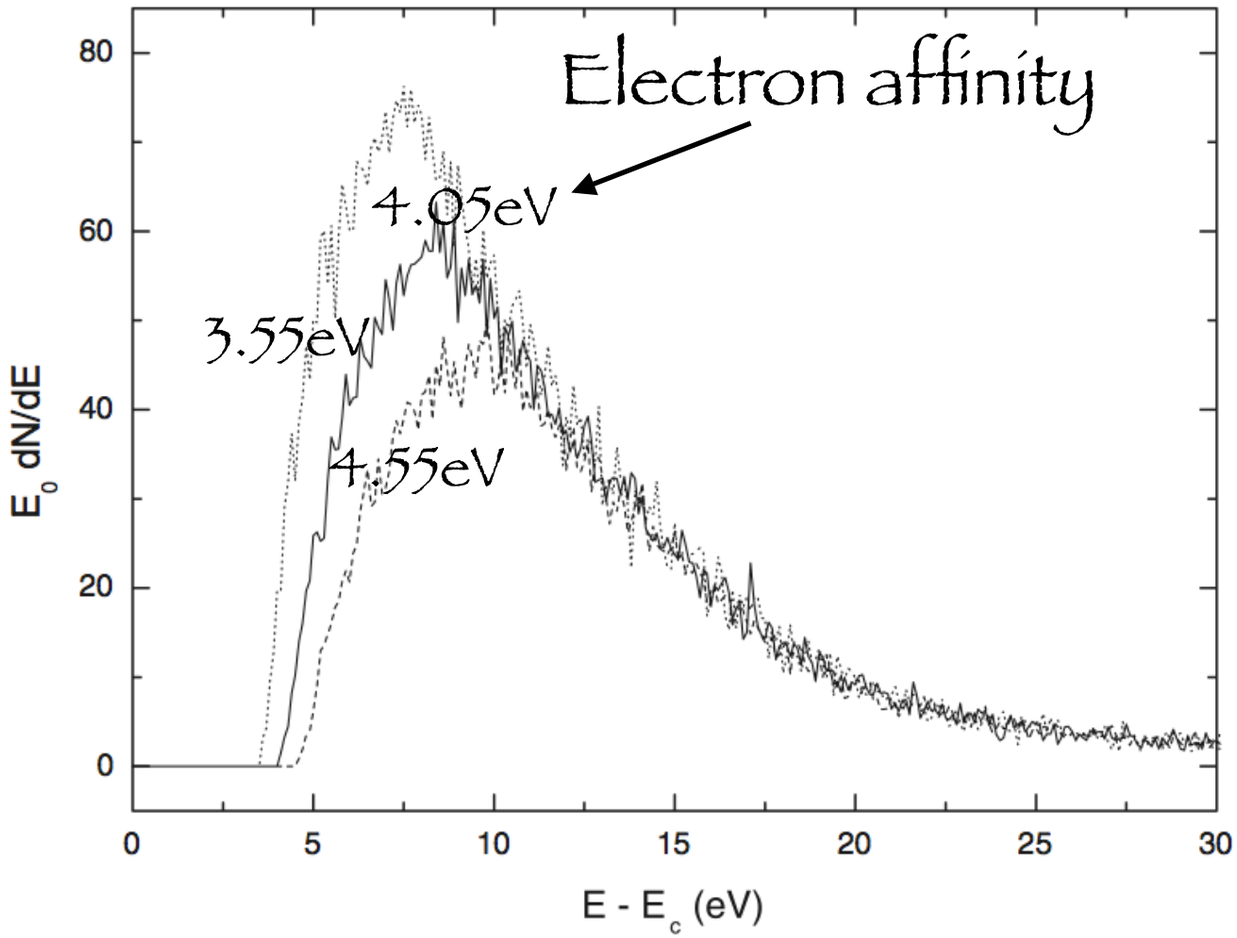

Monte Carlo simulation of the energy distributions of the secondary electrons emitted by a Si target

M. Dapor, B. Inkson, C. Rodenburg, J.M. Rodenburg, EPL, 82 (2008) 30006

Line-scan

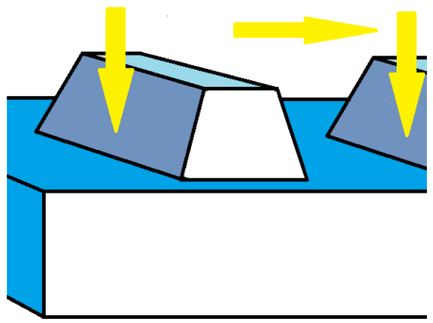

A material (e.g. Si, SiO2, PMMA) with trapezoidal cross-section on silicon substrate

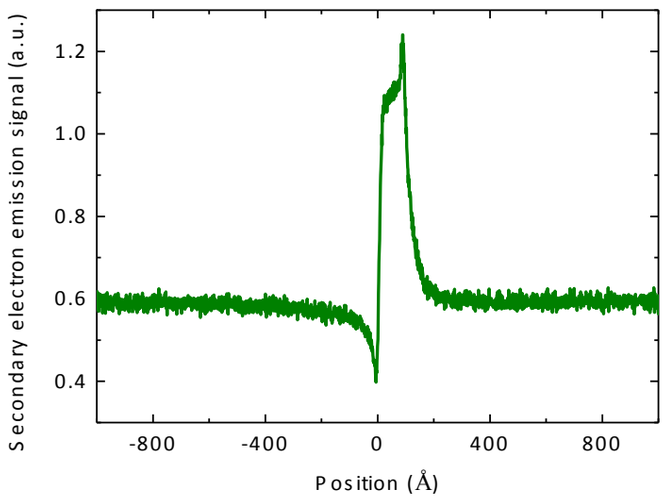

Single Si step with side wall angle equal to 10° (E0=700eV)

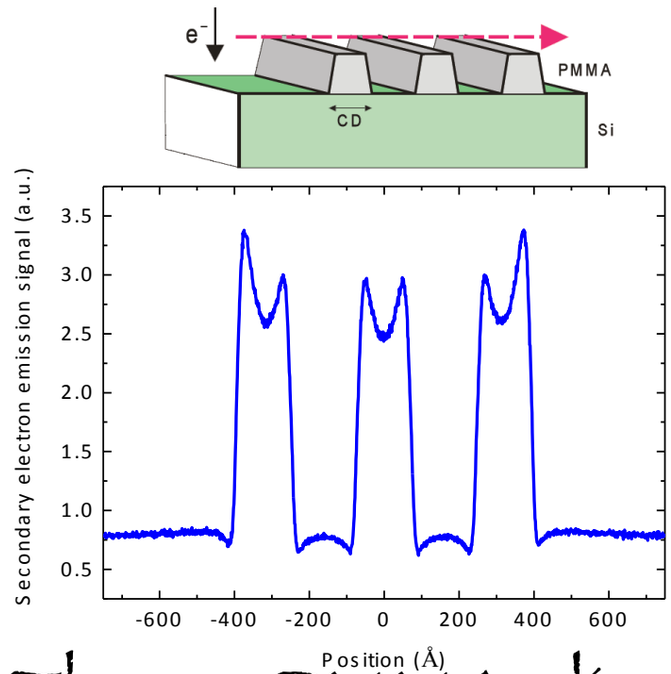

Three PMMA lines (height: 200Å, bottom width: 160Å , top width: 125Å, side wall angle: 5°) (E0=500 eV)

A. Koschick, M. Ciappa , S. Holzer, M. Dapor, W. Fichtner, Proc. of SPIE *7729* (2010) *77290X-5*

Ion beam cancer therapy

We wish to minimize the effects of the irradiation on the healthy tissues near to the diseased cells.

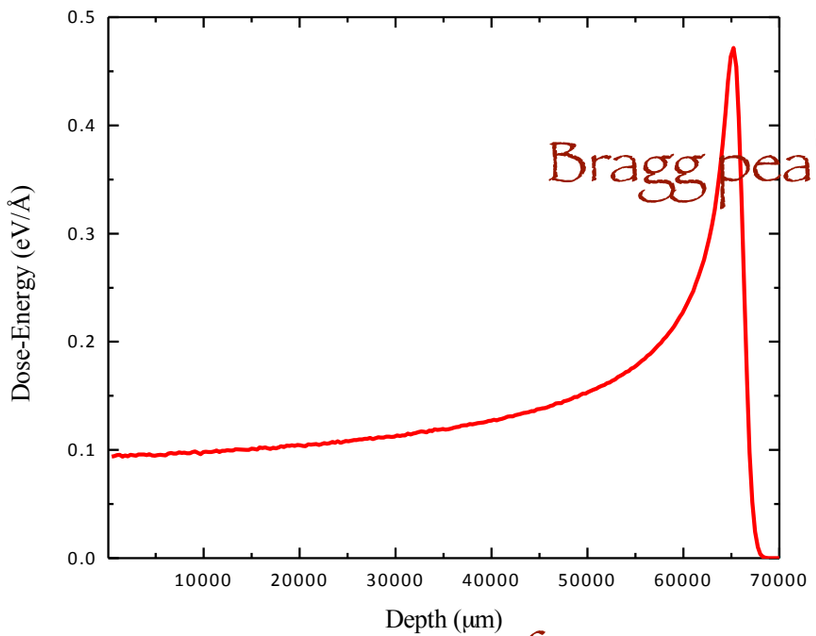

Dose-Energy of 100 MeV protons in PMMA (I. Abril et al.)

The shower of secondary electrons produces damage in the biomolecules (for example, due to dissociative electron attachment, DEA).

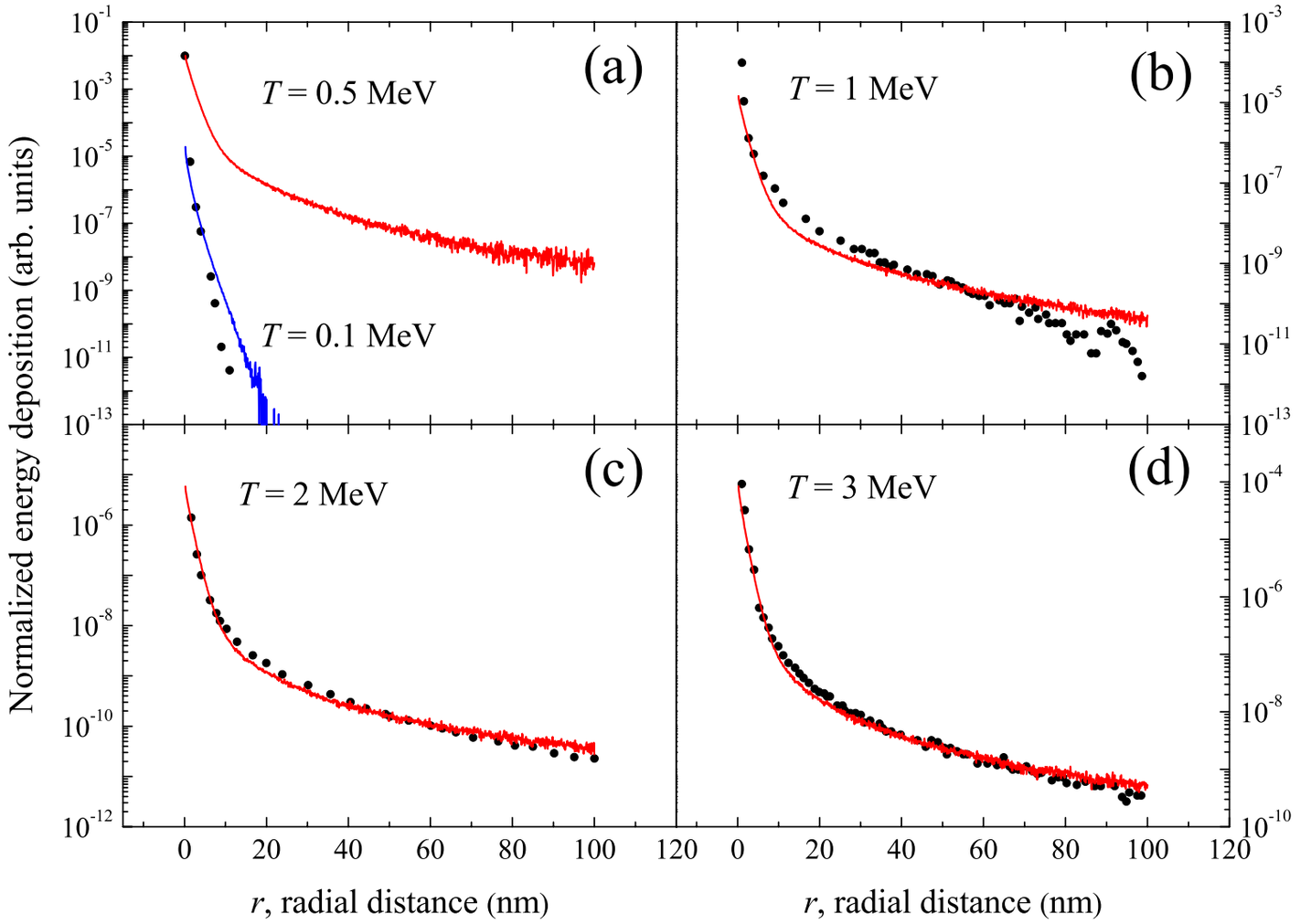

Energy deposited radially by secondary electrons along the track of 0.5MeV, 1.0MeV, 2.0MeV and 3.0MeV proton beams incident on PMMA

M. Dapor, I. Abril, P. de Vera, R. García-Molina, Phys. Rev B 96 (2017) 064113

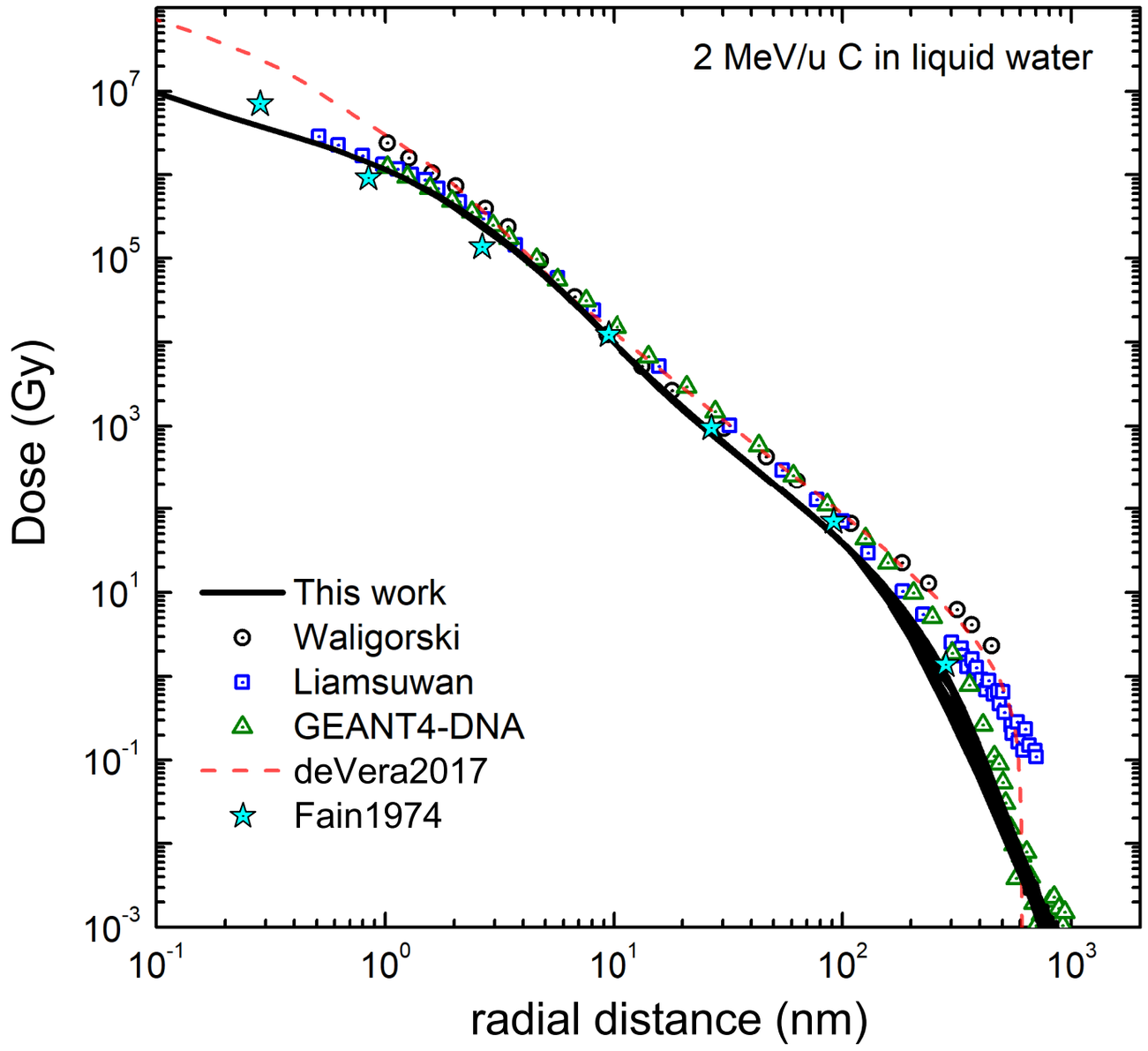

Dose deposited by 2 MeV/u carbon ions in liquid water, as a function of the radial distance from the ion path

P. de Vera, S. Taioli, P. E. Trevisanutto, M. Dapor, I. Abril, S. Simonucci, R. García-Molina, Int. J. Mol. Sci. 23 (2022) 6121

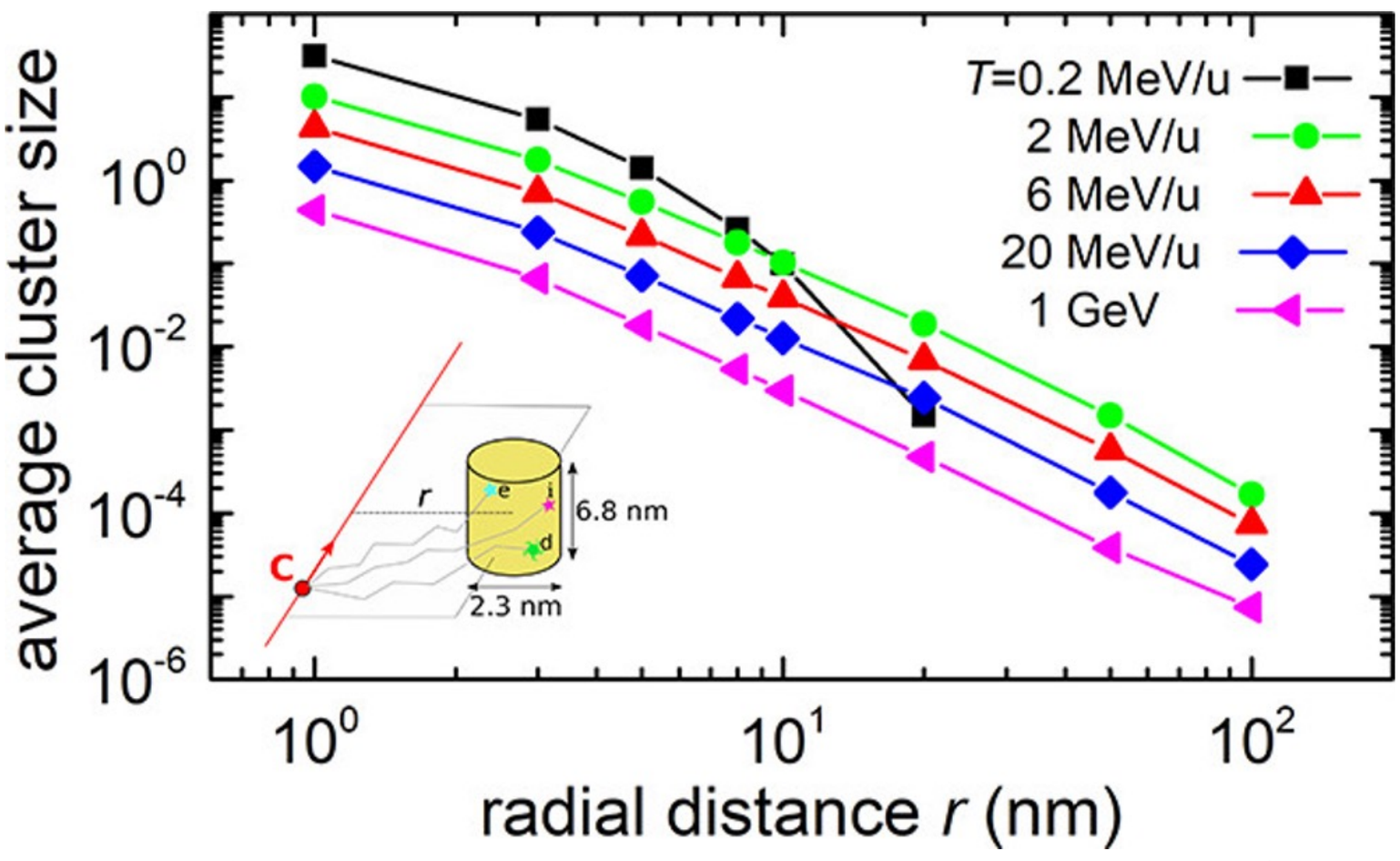

Average cluster size of damaging events in a sensitive volume of liquid water with a dimension of two DNA turns as a function of the radial distance r from the ion track for different values of the carbon-ion energy T. The inset depicts a scheme of the nanometric cylinder used in the scoring of the following damaging events: excitation (e), ionization (i), and dissociative electron attachment (d).

S.Taioli, P. E. Trevisanutto, P. de Vera, S. Simonucci, I. Abril, R. García-Molina, M. Dapor, The Journal of Physical Chemistry Letters 12 (2021) 487

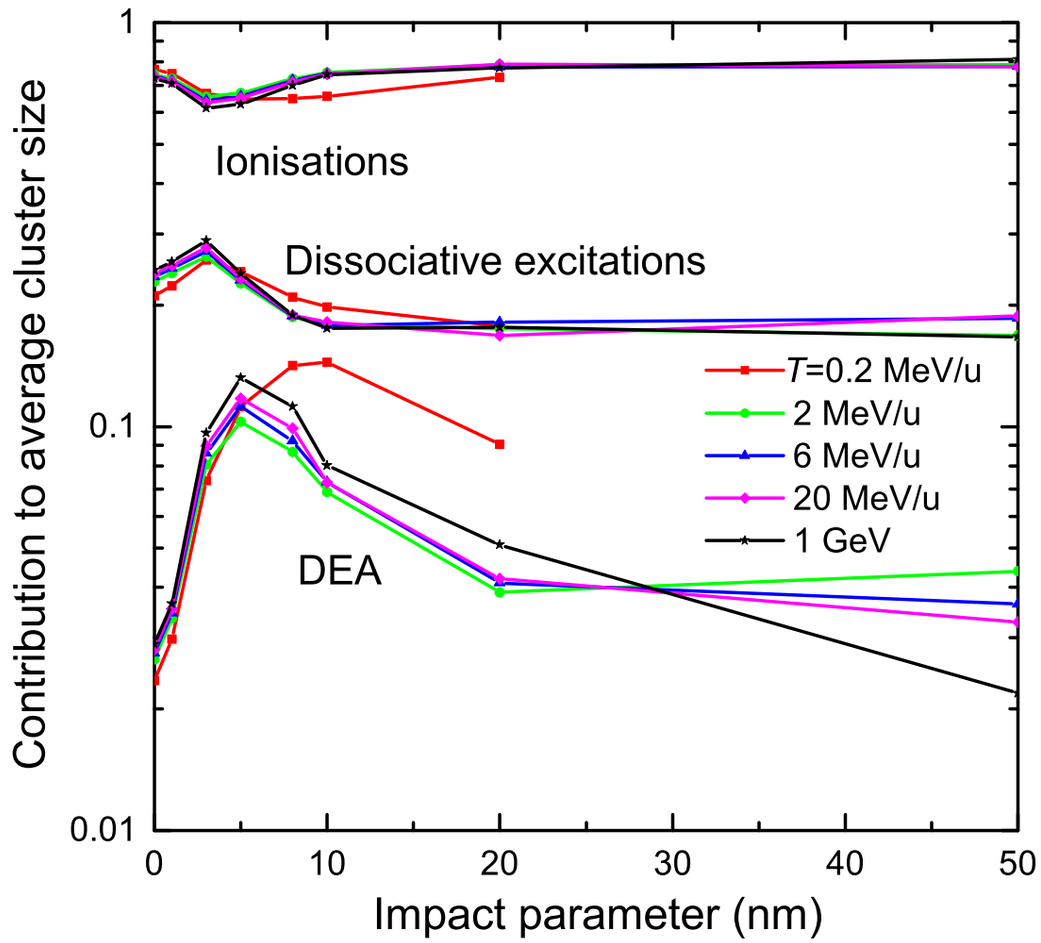

Fractional contribution to the average cluster size in a cylinder with a dimension of two DNA turns due to ionization, excitation (with only 40% of them leading to molecular dissociation), and dissociative electron attachments events for several carbon-ion kinetic energies and impact parameters.

P. de Vera, S. Taioli, P. E. Trevisanutto, M. Dapor, I. Abril, S. Simonucci, R. García-Molina, Int. J. Mol. Sci. 23 (2022) 6121

P. Sigmund, Particle Penetration and Radiation Effects (Springer 2006)

R. F. Egerton, Electron Energy-Loss Spectroscopy in the Electrons Microscope, 3rd edn (Springer 2011)

M. Dapor, Transport of Energetic Electrons in Solids 3rd edn (Springer 2020)

M. Dapor, Electron–Atom Collisions: Quantum-Relativistic Theory and Exercises, Berlin, Boston: De Gruyter, 2022.

Thank you for your attention!